batteries

MDPI

Invited Review

Advances in Additive Manufacturing Techniques for Electrochemical Energy Storage

Adrija De[1], Brindha Ramasubramanian[2,3], Seeram Ramakrishna [3#] and Vijila Chellappan[2*]

[1] Department of Metallurgical Engineering, IIT-BHU, Varanasi, India; adrija.de.met20@itbhu.ac.in (A.D.)
[*2] Institute of Materials Research and Engineering (IMRE), Agency for Science, Technology and Research (A*STAR), #08-03, 2 Fusionopolis Way, Innovis, Singapore, 138634, Republic of Singapore brindharamasubramanian@u.nus.edu (B.R.)
[#3] Centre for Nanotechnology & Sustainability, Department of Mechanical Engineering, National University of Singapore, Singapore, 117575, Singapore

* Correspondence: c-vijila@imre.a-star.edu.sg (V.C.)* | seeram@nus.edu.sg (S.R.)#

Abstract: The increasing adoption of additive manufacturing, also known as 3D printing, is revolutionizing the production of wearable electronics and energy storage devices such as batteries, supercapacitors, and fuel cells. This surge can be attributed to its outstanding process versatility, precise control over geometrical aspects, and potential to reduce costs and material waste. In this comprehensive review, major AM processes like inkjet printing, direct ink writing, fused deposition modelling, and selective laser sintering/melting along with possible configurations and architectures, are elaborately discussed for each bespoke energy storage device. The application of 3D-printed energy storage devices in wearable electronics, IoT-based devices, and electric vehicles are also mentioned in the review. The role of AM in facilitating the production of solid-state batteries has also revolutionized the EV industry. Recent progress in the field of additive manufacturing of energy systems with solid electrolytes and potential future directions such as 4D printing to incorporate stimuli-responsive behaviour in 3D-printed materials, biomimetic design optimization, and additive manufacturing of energy storage systems in a micro-gravity environment have also been highlighted. Extensive research and continuous progress in this field is expected to enhance the long-term stability, industrial scalability and electrochemical performance of 3D-printed energy storage devices in future.

Keywords: Additive Manufacturing; Energy Storage; Batteries; Supercapacitors; Fuel cells; Solid-state Batteries; Wearable electronics; Customizable electrodes; Microfabrication

Citation: To be added by editorial staff during production.

Academic Editor: Firstname Lastname

Received: date
Revised: date
Accepted: date
Published: date

1. Introduction

1.1. Overview

In today's rapidly evolving electrochemical energy storage (EES) sector, marked by vast market opportunities and optimistic prospects with present market cap of 104.31 billion dollars and predicted compound growth rate of 15.8% from 2023 to 2030[1], there is a crucial need to incorporate 3D-printed designs and flexible electrodes for integrating LIBs to wearable technologies. This mandates the exploration and adoption of state-of-the-art manufacturing techniques, such as additive manufacturing (AM) and precision deposition (PD) , that possess the capacity to adeptly accommodate intricate LIB design and ensure their seamless multi device integration [2–4]. Conventional manufacturing techniques, due to their multi-step nature, lack flexibility in design and efficiency in creating complex structures. These methods result in material waste, increased production costs, and environmental concerns arising from the use of hazardous chemicals like mercury in traditional batteries[2,3]. As an effort to overcome these challenges, a myriad of

AM techniques exists at present times, which differ among themselves with respect to outcomes, principles and embodiment [2–4]. Unlike conventional subtractive manufacturing techniques where parts are machined to obtain a near-net shape product, AM involves deposition in successive layers of material according to the STL(stereolithography) file design, thus yielding a net shape product with a low buy-fly ratio (raw material weight :final processed product weight)[5,6]. This not only reduces operation time but also minimizes the wastage of material to a large extent, making AM a genuinely sustainable process. While AM was first solely used for rapid prototyping, it is currently evolving into a platform for the industrial production of finished goods with widespread applications in the aerospace, automotive, medical, and, significantly, energy-related areas [6]. With regard to batteries in particular, AM can offer explicit control over the necessary geometry to permit complex ion/electron transport while enduring mechanical stability and safety [7].

The first 3D printed object (a teacup) was made by Charles Hull in 1983 using the stereolithography technique[11]. Following his invention, over 25 AM processes have been developed like laser engineered net shaping (LENS),Directed Energy Deposition (DED), Selective Laser Sintering (SLS),etc., though most of them cannot be applied at an industrial scale[2,8]. The classification of AM processes is a tedious task, with each process being differing with respect to physical state of the starting material, equipment, principle, methodology of formation of this product and medium used for processing. Based on the type of material used, they are further classified into solid (Laminated Object Manufacturing (LOM), Fused Deposition Modelling (FDM), Wire and Arc Additive Manufacturing (WAAM) and Electron Beam Free Form Fabrication (EBF3), liquid (Stereolithography(SLA), Direct Light Processing (DLP) and Polyjet Printing) or powder-based (Selective Laser Sintering (SLS), Electron Beam Melting (EBM) and Laser Metal Deposition (LMD))[9] . This ambiguity was solved in 2015 when ISO assumed the ASTM (American Society for Testing of Materials) categorization with its new standard ASTM F2792, modifying the ISO 2010 standard [10] , thus classifying the processes according to the following categories as shown in Figure 1 that are the foundation of every manufacturing process:

1. Material
2. Energy
3. Machine and Tool
4. Technology

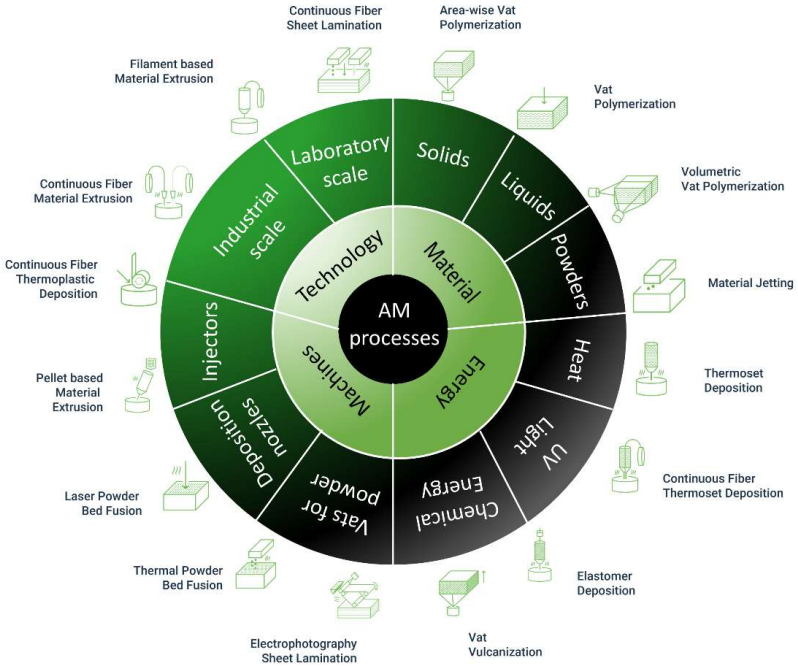

Figure 1: Classification of AM techniques according to 2015 ASTM standard (Figure modified from [11])

However, the six major AM processes according to 2012 ASTM classification [12] are: vat photopolymerization, binder jetting (BJ), material jetting(MJ), laser power bed fusion, material extrusion processes and sheet lamination. Additive manufacturing techniques are classified into distinct methodologies: Directed Energy Deposition (DED), Vat polymerization (e.g., Stereo-lithography, digital light processing), Material jetting (MJ), Binder Jetting (BJ), powder bed fusion (PBF), Material extrusion (e.g., Fused Deposition Modelling), and sheet lamination. Vat photopolymerization, SLA and DLP involves layer-by-layer deposition using UV exposure [13,14], while MJ imitates 2D inkjet printing [15]. BJ employs powdered material and liquid binders for powder sintering [16], PBF fuses layers with lasers or electron beams, and FDM deposits heated material. Sheet lamination welds metal sheets ultrasonically at low temperatures [16].

Some of the above-mentioned AM processes are illustrated and explained in Figure 2.

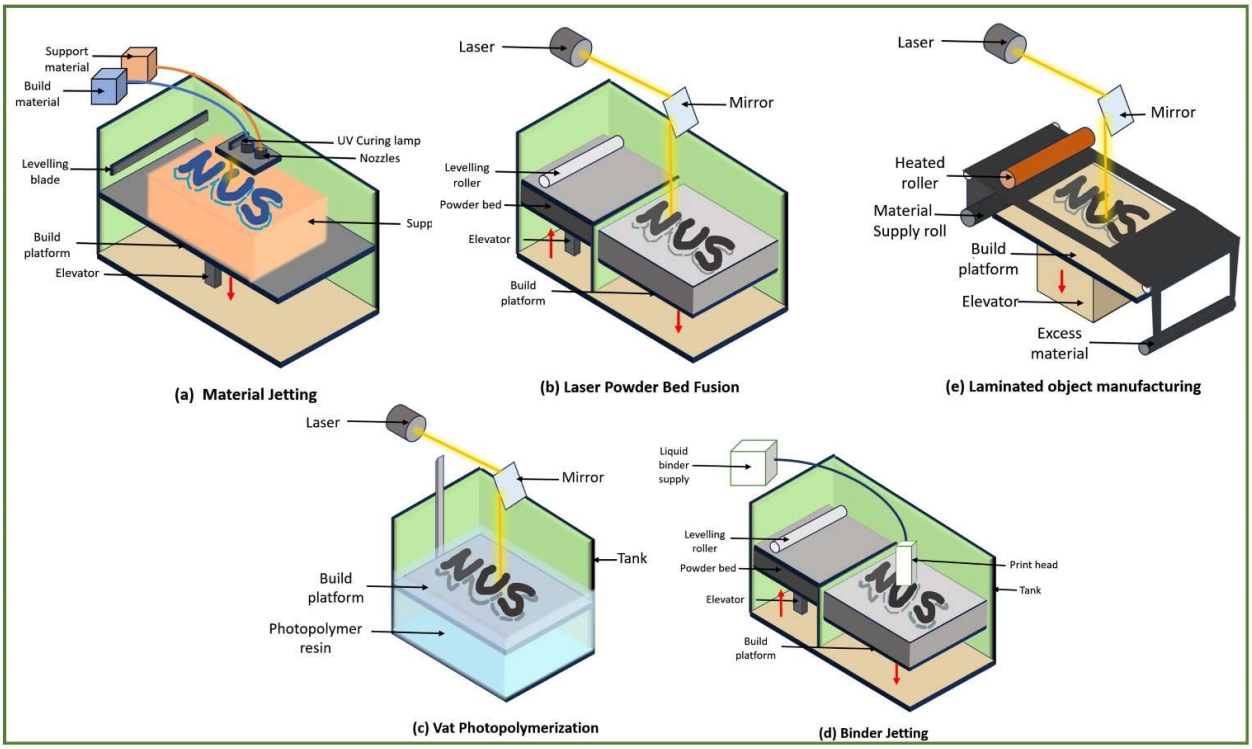

Figure 2: Major additive manufacturing processes. **(a)** MJ involves depositing the build material and support material via nozzles. The build material is then cured by UV rays to yield the final shape. In all the processes, the build platform gradually descends to help in successive layer formation. **(b)** In the LPBF process, the base powder is sintered by selectively fusing it with laser beam. **(c)** In the VP process, the photopolymer is cured by laser beam to obtain the desired structure. **(d)** BJ works on the same principle as LPBF, except for the fact that the powder particles are sintered here using liquid binders. **(e)** In LOM, a continuous supplied heated metal sheet is selectively cut by laser beam to get the final product.

Traditional battery production involves preparing electrolytes and electrodes, assembling cells, and conducting sealing and testing. In commercial LIBs, the cathode includes $LiNiMnCoO_2$, $LiCoO_2$, $LiFePO_4$ mixed with polymer binders such as PVDF, PVP, PVA, and metal oxides, graphite. The anode is usually Li metal, Si, graphite and electrolyte. Brass nails serve as current collectors during sealing, along with plastic seals. The traditional processes lead to material wastage and is also time-consuming, though they have good industrial scalability at present. Both Li and cobalt possess high risk of resource scarcity[17]. The process involves slurry mixing where a binder, active material and other conductive additives are mixed to form a slurry. The next step involves coating and drying the slurry in the form of thin sheets onto the current collectors and cutting the electrodes out of it[18,19].

This process applies to nickel-cadmium batteries which contain nickel oxide, cadmium oxide and metallic nickel where both nickel and cadmium are toxic materials, restricting its use. AM can also facilitate in exploring alternate materials for such batteries[20].

For aluminum electrolytic capacitors, production starts with chemically etched anode aluminum foil coated with Al_2O_3 for dielectric properties. Anode and cathode foils, insulated by paper, are coiled and housed, followed by addition of electrolytes. They are manufactured by etching and slitting the aluminium foils, which is accompanied by rolling them into cylindrical electrodes and impregnating them with an electrolyte and sealed[21].

In fuel cell energy storage systems, proton exchange membrane (PEM) fuel cells are prominent, especially in automotive use. These cells consist of a proton exchange polymer membrane, two catalyst layers (Mn, Fe, graphite, Ru, Pt, and Ag), porous gas diffusion layers, bipolar plates, and seals. Plates and membrane stack alternately as anodes and cathodes, fortified by flow channels and collectors. This stack forms a functional fuel cell system. Because each MEA produces no more than 1 V, they are typically stacked to achieve the required voltage, with each cell split by bipolar plates and gaskets to ensure a tight seal[22,23].

- Fabrication and rapid prototyping of complex architectures with high control accuracy becomes possible[24].
- Precise control on the shape, size and thickness of the electrodes [25]
- Enhanced areal capacitance is attained by employing on-chip Energy Storage and Delivery Systems that have been optimized to encompass a range of thicknesses, spanning from hundreds of nanometers to millimeters[26].
- Additionally, it can offer direct integration of EESDs with outside electronics, eliminating the need for device assembly and packaging stages[24].
- 3D printing or AM reduces material waste to a large extent as discussed earlier, and also saves a lot of time.

3D-printed batteries are light-weight, have design flexibility, energy and power density and demonstrate improved performance as compared to their 2D counterparts. The global AM-based battery market is projected to be valued at 675.9 million USD by 2031. The solid-state batteries are 33% lighter than LIBs and conventional batteries, a significant characteristic that has the potential to boost the e-mobility market. The market share for solid-state batteries and graphene FDM-based batteries is expected to expand at a CAGR of 25.1% and 23.9% respectively in the next 10 years[27]. FDM, DIW, Template-assisted electrodeposition (TAE), IJP, AJP (Aerosol Jet Printing) and SLA are some of the major AM techniques used recently used for 3D printing batteries. SLA and holographic lithography are laser-based AM techniques used for fabricating periodic geometries, while TAE is mainly utilized for developing macroporous batteries with optimizable pore sizes and nanostructured electrodes. AJP, a contactless process identical to DIW, is a relatively new technique and has not been explored much for AM of batteries. Other AM methods mentioned above have been discussed in detail in Section 3.1. Although LTO and LFP are major electrode constituents, other materials like graphene oxide (GO), reduced GO (rGO), carbon nanotubes and nanofibers are also added to improve the electrical conductivity of 3D-printed electrodes[26]. Majority of recent research regarding 3D-printed batteries emphasizes on exploring various electrode and electrolyte materials, and increasing the scalability of production by reducing costs associated with printing equipment and conditions.

The following review will focus on various AM techniques for EESDs, especially batteries, capacitors, supercapacitors and fuel cells. The major AM techniques like IJP, FDM, DIW, SLS and LOM are discussed elaborately for each EESD, citing recent works and new materials being explored for each process. When compared to other reviews on similar topic, this review also discusses AM of fuel cells, design aspects of each EESD and future directions like 4D printing, AM on Moon and Mars, which makes it novel and comprehensive. The review will consider the potential advantages and limitations of AM for EESDs, including factors such as design flexibility, material selection, and manufacturing scalability. Our objective is to evaluate the current research landscape in additive manufacturing of ESDs where we will be focusing on solid electrolytes and wearable electronics, and to identify areas where further research is needed to advance the field.

1.2. Methodology

While crafting this comprehensive review on the recent advances in AM techniques for EESDs, we placed a significant emphasis on academic literature as our primary information source. We heavily relied on scholarly articles and research papers that served as a foundation of our study and complemented our findings with insights from blog posts and industry reports to provide practical, real-world examples and case studies. This approach ensured that our review was based on rigorous academic research and also demonstrated the practical applications of 3D printing in the energy storage industry. Initially, recent review articles were referred to get an overview of the topic and structure the basic outline of the review. The initial survey commenced with a pool of over 250 sources, a selection process that subsequently narrowed down to approximately 150 sources. This filtering was guided by the following criteria: 1. Published after 2015; 2. Emphasized on the role of 3D printing in EESD fabrication; 3. Had results and outcomes that contribute significantly to the advancement in this field. In this review, an overview of AM processes involved and highlights of recent works were summarized and presented for each category of EESD (batteries, supercapacitors and fuel cells). Recent articles published in the last three years were referred for applications, recent advances and future directions in this field.

This review is structured as follows: Section 2 provides a historical insights into the evolution of 3D printing process and materials for all EESDs. Section 3 discusses the AM processes used and recent studies in brief details for each EESD. Section 4 delves into an extensive discussion on the properties and performance of 3D printed EESD with different designs, architectures and configuration. Section 5 focuses on elucidating the various application in this field. Section 6 opts a forward-looking perspective by focusing on the recent advances and contemplating future directions, followed by a succinct summary and conclusion in Section 7.

2. Historical Context

If inkjet-printing (IJP) can be considered an AM method, 3D-printed LCO cathodes were fabricated by Prof. Jiang's research group in 2008 [28] and can be considered a stepping stone for the 3D-printed EESD revolution. One of the earliest advancements in the field of 3D-printing LIBs was done by a group of researchers from Harvard University, University of Illinois- Urbana Champaign and Korea Advanced Institute of Science and Technology (KAIST) in 2013 as shown in Figure 3.(a). Li-ion microbatteries were 3D printed using Direct Ink writing (DIW), where $Li_4Ti_5O_{12}$ (LTO) and $LiFePO_4$ (LFP) inks are deposited over interdigitated gold current collector patterns and finally packaged using a poly(methyl methacrylate) (PMMA) preform [29].

In 2014, Chen Zhao et al. from the University of Wollongong additively manufactured Ti_6Al_4V electrodes using the SLM technology as seen in Figure 3. (c), which is almost identical to the LPBF process. The fabricated Ti electrodes were further used as a platform to build a solid state supercapacitor by filling it with a poly(vinyl alcohol) (PVA)-H_3PO_4 polymer electrolyte. Moreover, the 3D printed supercapacitor demonstrated performance comparable to that of supercapacitors manufactured by conventional lithography method [30]. A group of scientists from University of Illinois-Urbana Champaign in 2015 combined 3D holographic lithography with 2D lithography to fabricate mesostructured Li-ion microbatteries consisting $LiMnO_2$ cathodes and NiSn anodes on a 3D porous current collector. Compared to the DIW based microbatteries developed earlier [29,31,32], this technique generates defect-free periodic structures in a one-step beam exposure. The complexity and periodicity of the fabricated structures can be further controlled by varying the exposure conditions and beam patterns [33]. After these innovations, there was increased emphasis on the creation of better ink materials improving the printing capabilities. Fu et al. in 2016 incorporated graphene oxide (GO) flakes in LTO and LFP inks, whose concentration can be varied to yield diverse and complex architectures[31]. In the same year, Kohlmeyer et al.[32] proposed the formulation of current collector-embedded electrode

inks composed of LTO,LFP, and $LiCoO_2$ (LCO) with a 3D network of carbon nanofibers, thus developing composite batteries.

As additive manufacturing of EESDs gained momentum, all the known AM processes discussed above were explored for the fabrication of more efficient EESDs with an aim to improve the ease of printing, aspect ratio and electrical conductivity. The growing interests around graphene and carbon nanotubes, which possessed promising improvement in the electronics sector back then posed a new challenge when it comes to DIW based EESDs as the evaporation of solvent introduced stresses in the graphene film and restricting its commercial scalability due to the possibility of manufacturing only thin films. Moreover, polymers used in AM processes have poor ionic conductivity. In 2017, Azhari et al. developed thick graphene electrodes for supercapacitors using the binder-jetting powder bed process (Figure3.(d)), which helped in eliminating the need for a solvent [34]. LOM-based 3D laser-induced graphene foams were fabricated by Luong et al. [35] and were used as self-standing electrodes for Li-ion capacitors, eliminating the need of a binder and a current collector altogether.

In 2018, the Fused Filament Fabrication (FFF) technique was explored to fabricate Li-ion batteries (LIBs) with an aim to facilitate their use as a structural component. Reyes et al. infused poly(lactic acid) (PLA) with a mixture of ethyl methyl carbonate, propylene carbonate and $LiClO_4$ for the fabrication process [36]. It was also found that highly complex micro-to mesoscales 3D architected electrodes can be easily fabricated by DLP method [37]. Nevertheless, the application of Digital Light Processing (DLP) has not been extensively investigated and studied for this particular objective, primarily due to the inherent limitation of the resin materials employed in this process. These materials often possess inadequate conductivity, resulting in the production of non-conductive polymers as the end product. While one side of research was focused on examining the feasibility of different AM processes like FDM, DLP, SLA, etc., the other side was focused on developing more complex hierarchically cellular lattices [38] using 3D printing that would improve the areal capacitance and conductivity of batteries and capacitors. Though LIBs are the most researched types of EESDs for 3D printing, recent years have seen a rise in AM processes for other forms of EESDs like Na-ion batteries, zinc batteries and MXenes-based supercapacitors (Figure 3.(f)) [39].

Unlike batteries and supercapacitors, the multilayered structure of PEM and solid oxide fuel cells (SOFCs) makes them an ideal candidate for 3D printing as separate layers can be printed and stacked together to form a final cell. Early 3D printed fuel cells date back to 2007s when IJP (Figure 3.(a)) was used to deposit catalyst materials onto GDLs [40], unlike the conventional screen printing method which was time consuming. Though direct printing of polymer and ceramic [41] electrolytes for FCs have progressively advanced this research field, IJP is not suitable for printing complex architectures with high aspect ratios, as was the case with batteries and supercapacitors. In the upcoming sections, we will delve more into the materials, methods, and drawbacks of the AM processes used for EESD fabrication discussed above.

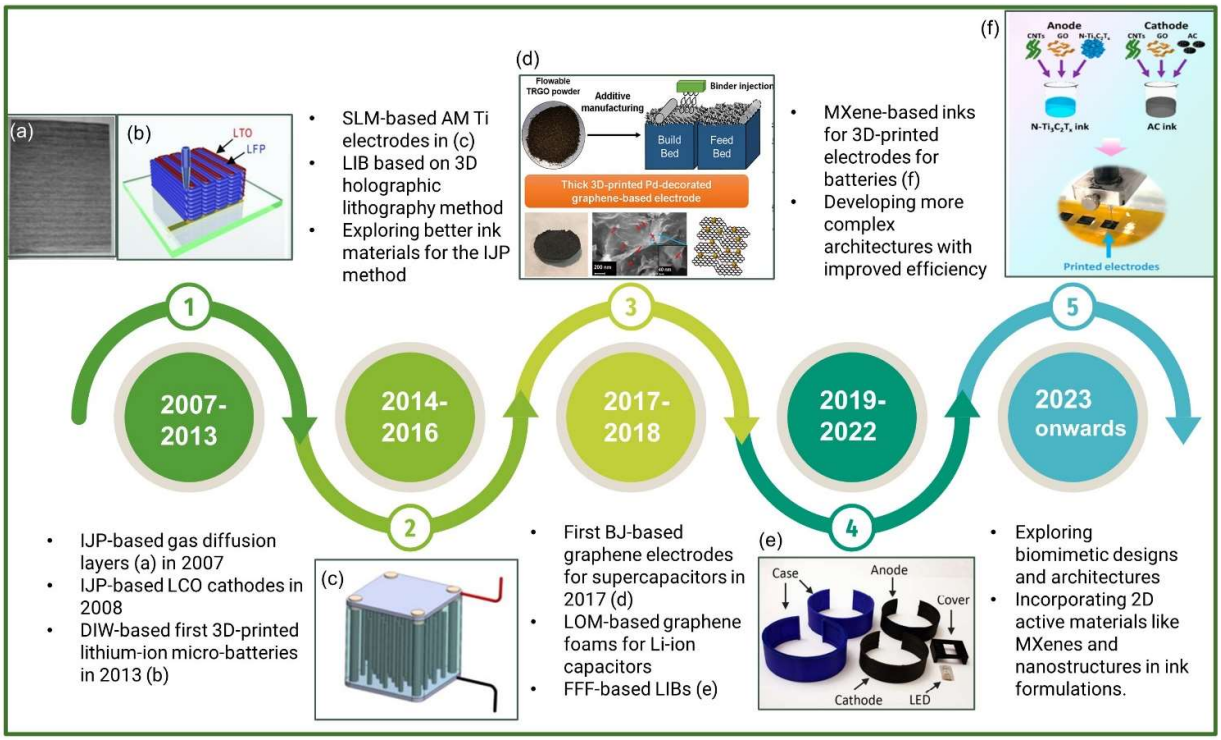

Figure 3: Timeline depicting development of AM processes for EESDs. **(a)** IJP-printed catalyst layers. Reprinted with permission from Taylor et al. [40] Copyright © 2007, Elsevier B.V. **(b)** DIW printed LIBs with LTO and LFP inks. Reprinted with permission from Sun et al. [29]Copyright © 2013, John Wiley & Sons, Inc. **(c)** Interdigitated titanium electrodes. Reprinted with permission from Zhao et al. [30] Copyright © 2014, Elsevier B.V. **(d)** Fabrication of BJ-based graphene electrodes. Reprinted with permission from Azhari et al. [34] Copyright © 2017, Elsevier B.V. **(e)** FFF-based components for fabrication of LED bangle. Reprinted with permission from Reyes et al. [36] Copyright © 2018 American Chemical Society (f) Electrode fabrication using MXene inks. Reprinted with permission from Fan et al. [39] Copyright © 2020 American Chemical Society.

3. Materials and Methods

Most of the EESDs are fabricated using DIW, IJP, SLA, and FDM processes. The selection of appropriate materials and methods are crucial for the development of an efficient EESD having electrical conductivity and areal capacitance comparable or even better than those manufactured by conventional techniques. We would be discussing each of the processes in detail for each EESDs discussed above (batteries, capacitors, supercapacitors and fuel cells), highlighting the materials used and the resulting efficiency of the final EESDs.

3.1. Additive Manufacturing of Batteries

3.1.1. Direct Ink Writing (DIW)-based batteries

DIW is an extrusion-based AM technique [42] that builds objects by depositing ink layer-by-layer or paste materials in a precise pattern using a computer-controlled nozzle. The ink or paste is dispensed from the nozzle in a carefully regulated manner, facilitating the formation of the desired shape, while the material undergoes solidification or cross-linking to establish a stable structure. This AM process offers versatility, as it accommodates various materials such as metals, polymers, ceramics, and composites. The process enables the creation of complex structures with intricate geometries and can produce high-resolution and high-precision components. DIW can also fabricate multi-material and gradient structures, offering the possibility of integrating different functionalities or gradually transitioning properties within a single printed component. During its flow

through the nozzle, ejection from the nozzle and finally depositing on the substrate, the rheology and printability of the ink plays a crucial role at each step. Generally, an ink is only regarded as printable if it can be extruded from the nozzle as continuous filaments and has the ability to build structures identical to the CAD model. As discussed earlier, DIW is mostly applied to microbatteries, requiring the use of micronozzles for ink deposition. In such cases, the shear-thinning behavior (reduction in viscosity with an increase in shear rate) can aid in reducing extrusion pressure and increasing ink extrudability [43].

In DIW, the inks used are typically yield stress fluids. When subjected to a critical stress known as the yield stress, these fluids demonstrate attributes of both viscoelastic and elastic materials, displaying flow only when stress outstrips the yield point. For an ideal yield-stress ink, its properties should be exclusively dependent on the shearing rate, enabling it to swiftly restore its structural integrity once the flow ceases. It is crucial for the ink to recover quickly after its deposition to maintain accurate shape and prevent the structure from slumping[43]. It is important to note that although the ink is no longer subjected to high shear stresses when deposited from the nozzle, it still undergoes considerable deformation before it is finally deposited. The extent of stretching of the ink can be regulated by adjusting the ratio between the printing speed and extrusion rate. Colloidal dispersions, emulsions and polymeric gels are some of the yield-stress fluids that are used as inks due to their packed microstructure, owing to their attractive or repulsive interactions among their constitutive elements[44] . Energy-storage based materials like LTO, LFP, graphene and carbon nanotubes (CNTs) are further added to these materials to yield functional inks. For example, Kim et al. [45] developed an ink suitable for DIW by formulating a mixture composed of polyvinylpyrrolidone (PVP)-wrapped multiwalled carbon nanotubes (MWCNTs). The ink was composed of 7% MWCNTs and 17% PVP in water, possessing rheological properties desired for DIW. The addition of PVP helped in preventing agglomeration and clogging of the printing nozzle and MWCNTs increased the functional properties such as electrical conductivity, high energy density and mechanical integrity. The authors reported an impressive electrical conductivity of 2540 S m^{-1}. Several rheological mathematical models exist to describe the flow behavior of inks[46]:

- Herschel-Bulkley Model: $\tau = \tau_y + K\dot{\gamma}^n$ [44]

Where K is the viscosity parameter, τ the shear stress, τ_y the yield stress and n the flow index. This model highlights the importance of threshold yield stress below which ink cannot flow. One of the major drawbacks of this model is its inability to predict the viscoelastic or elastic flow behavior below yield point and cannot be used for direct comparison of various inks.

- M' Barki model: $\sigma_y \geq \gamma R^{-1} + \rho g h$ [47]

Where γ is the surface tension of the suspension, σ_y the dynamic yield stress, R the nozzle diameter and $\rho g h$ the gravitational force acting on the deposited filament. This model establishes a criterion for minimum yield stress required to avoid slumping.

As mentioned earlier, the inks for AM of EESDs contain two major components: an active material to impart the functional properties related to EESDs and inactive, non-conductive species like fillers, binders, surfactants, stabilizers and viscosifiers to enhance the printability and extrudability of inks. These inactive components should be removed at high temperatures resulting in an increase in the post-processing cost [46]. The most common form of functional fillers is nanomaterials in colloidal form like nanowires, nanotubes, nanoflakes, and quantum dots[46]. These nano-fillers impart unique electrical properties and avoid clogging as their sizes are negligibly smaller to the nozzle diameter[46]. Binders are added to improve adhesion with the underlying substrate and solvent is added to impart fluidity to the ink. Kohlmeyer et al. [32](as discussed in section 2) used poly(vinylidene fluoride) (PVDF) as an organic solvent and binder with LTO, LCO, LFP with a 3D network of carbon nano-fibers (CNFs) as active materials. It was observed that CNFs reduced the ink's shear-thinning behaviour, thus reducing the extrudability of inks to some extent.

Though LTO, LFP, LCO are the most common active materials used in fabrication of Li-ion based EESDs, research on other active materials such as graphene-based materials and MXenes have recently gained momentum. Epoxy, hydroxy and carboxyl groups in graphene oxide (GO), a derivative of graphene, are responsible for its high dispersibility in water, even at very high concentrations. Lacey et al. used stable dispersions of highly porous 2D graphene oxide (GO) in water without the use of binders or additives, possessing excellent shear-thinning behavior for the fabrication of complex 3D architectures. Here, the aqueous ink was used to manufacture lithium-oxygen (Li-O2) cathodes, where the trimodal porosity of the ink enhanced the areal discharge capacity of electrodes by 63-fold due to increased electron transport [48]. However, despite its versatility and simplicity, GO-based inks have limited electrical conductivity and exhibit capacitive behavior after reduction [46]. Fu et al. used LFP/GO and LTO/GO based composite inks for cathode and anode materials respectively and solid-state electrolyte inks to develop an all-component 3D-printed LIB. The ink was prepared by uniformly mixing LTO/LFP nanoparticles with GO sheets dispersed in an aqueous solution, generating well-aligned filaments along the extruding direction- a result of the shear thinning behavior imparted by GO. The AM-based LTO anode and LFP cathode demonstrated cyclic stability with specific capacitance of ~170 mAh g^{-1} and ~160 mAh g^{-1}, respectively. Moreover, the solid-state electrolyte composed of PVDF-co-HFP (hexafluoropropylene) eliminated the possibility of leakage and capacitive failure in batteries, as is the case for liquid electrolytes [31].

Similar to graphene, MXenes - another 2D material comprising of transition metal nitrides, carbides and carbonitrides, have been exploited in DIW-based energy storage applications extensively due to their unique properties like negative surface charge, excellent dispersion quality, faster ion intercalation between layers, high electrical conductivity and hydrophilicity. Moreover, unlike graphene, it does not require post-processing at high temperatures. MXenes synthesized via the wet chemical route typically have terminal -O,-F and -OH groups attached to them, which are responsible for their hydrophilic nature. These features make MXenes an ideal component in DIW inks and also eliminates the use of surfactants or binders [49]. Though 2D heterostructures based on MXenes were explored as a potential substitute for electrode materials [50], it was not until 2018 when Tang et al. [51] developed an MXene-based ink for Lithium-Sulphur (Li-S) batteries. An aqueous ink with nanoscale sulfur decorated on metallically conductive and MXene nanosheets ($S@Ti_3C_2T_x$) was developed with an aim to reduce the Li polysulphide shuttle effect and enhance the conductive properties of Li-S batteries. This fabricated ink could be used for many printing technologies and not only DIW printing. MXenes-based inks are mainly used for capacitors and supercapacitors (will be discussed in later sections), and using them for DIW-based batteries have not yet been explored.

Though DIW is a popular technique for fabrication of 3D-printed batteries, it has certain limitations. It presents specific challenges in the use of gel-based viscoelastic inks, requiring quite high enough storage modulus and yield strength. Additionally, a significant issue that needs to be addressed is the relatively fragile mechanical strength among the printed layers [26]. To overcome this obstacle and enhance the applicability of DIW in battery manufacturing, it is imperative to devote extensive efforts towards improving the technique.

3.1.2. Inkjet Printing (IJP)-based batteries

Inkjet printing (IJP), a sort of extrusion-based AM method comparable to DIW, has been widely used in the field of EES, from supercapacitors and batteries to electrochromic-based energy storage [57]. Droplet ejection, droplet spreading, and droplet solidification are the three basic steps of the process. The print head is initially positioned in the desired area, and ink droplets are ejected through the nozzles before being deposited into the substrate. These deposited droplets diffuse across the surface and join with other droplets to form a thin coating of liquid ink. Following that, the solvent in the ink evaporates, leaving behind solid elements on the substrate[57-[59][59]Like other AM processes, employs a

variety of materials, such as polymers, metals, and ceramics, expanding the potential for a wide range of applications. Furthermore, because it eliminates the need for complex equipment or moulds, it is a relatively quick and cost-effective procedure. In conclusion, IJP offers flexibility, precision, material adaptability, and cost efficiency, making it a beneficial technology in a variety of sectors [58],[60]

The relatively low printing resolution of 30 um in IJP imposes a limitation that renders it unsuitable for printing micro-electronic devices. However, it proves to be accurate for other planar energy devices such as micro-batteries, micro-supercapacitors and electrochromic. The printing resolution further depends on factors such as the rheological properties of jetted ink droplets, wettability of substrate, and printer quality [52]. The IJP process is classified into two categories based on the flow of droplets from the nozzle: continuous process, where the droplets flow in the form of a continuous stream, even when printing is not done and is relatively inefficient; and drop-on-demand (DOD) process, when droplets emerge from the nozzle only during printing, resulting in more efficient ink delivery. Droplets are generated in the fluid tube in a chamber behind the nozzle by propagating a pressure pulse, either thermally or piezoelectrically[53]. The piezoelectric mode is mostly preferred as it allows precise control over the pressure pulse and in turn, the velocity and size of the droplets.

IJP-based inks contain solvent, active materials and surfactant additives. The ink's rheological properties are characterized by the inverse Ohnesorge number Z (ratio of Reynolds number to the square root of Weber number) : $Z = \sqrt{\rho\gamma d}/\eta$ where ϱ is the density, η the viscosity, γ the surface tension and d the nozzle diameter. A Z value in the range of 1-10 ensures the formation of separated and stable droplets [53]. Just after the deposition, the printed patterns can be characterized by the density of droplets per unit length. These patterns are defined by the contact diameter (d) of the droplets, called footprint, and the distance between individual droplets (s). The control over droplet separation distance can be achieved by adjusting the printer's dpi settings[54]. The coffee-ring effect [55] after evaporation of the deposited droplets can be minimized either by particle shape control [56] or by composite ink engineering, both surfactants and solvents [57].

IJP-based batteries were one of the earliest forms of 3D printed EESDs, with this process being used to develop flexible organic radical battery cathodes by Janoschka et al. in 2013. The ink was composed of a conductive additive and polymer and a crosslinking agent (tetraphenylolethane glycidyl ether) and the printed electrodes could withstand almost 100 charging cycles [58]. Later, Delannoy et al. formulated a water-based LFP ink to develop cathode and lithium metal foil anode for a coin type half-cell. The printed electrode had an active mass loading of 0.35 mgcm^{-2}, and the full cell reported a discharge capacity of 63 mAh g^{-1} [59]. Another advantage that IJP offers is that it has been well-researched and a plethora of materials have been explored for IJP-based inks. Lawes et al. used commercial silicon nanoparticles as an active material to develop inkjet-printed silicon anodes for LIBs, unlike the usual LTO and LFP based electrodes. Among the four polymer binders the authors experimented on, poly(3,4-ethylenedioxythiophene)-poly(styrene sulfonate) (PEDOT:PSS) exhibited the most stable cycling for over hundred cycles at high discharge capacity, due to its excellent jetting properties, electrical conductivity and self-healing nature. Moreover, the binder acts like a conductive layer around the silicon nanoparticles which allows rapid electron transport while binding the electrode together [26,60].

As mentioned in Section 2, one of the earliest 3D-printed IJP devices was developed by Prof. Jiang's group in 2008[28], where thin film LCO cathodes were fabricated. Similar to DIW, LTO and LFP based materials are most widely used for formulation of inks for AM-based LIBs. The main obstacle they encountered was creating stable colloids with components that were electrochemically active and could be employed as inks for the ensuing IJP procedure. They created a stable suspension using nano LCO, conductive carbon black, monoethanolamine (used to modify pH), an industrial surfactant solution (as a dispersion to scatter LCO nanoparticles uniformly), and CMC solution (as a binder). The

discharge capacity of the generated LCO thin film electrodes at 384 μA cm^{-2} and at 192 μA cm^{-2} after 100 cycles were shown by experimental results to be 105 mAh g^{-1}[28,61]. In later years, IJP was also applied to fabricate solid-state electrolyte composed of ionogel [62], or flexible current collectors for LIBs [63].

Significant advancements have been made in enhancing the specific surface area of printed electrodes. An example of this progress is the development of a 3D freeze printing technique by the Li group [64] for manufacturing porous anodes for sodium-ion batteries. The precursor ink was made of ammonium thiomolybdate (ATM) and dispersed graphene oxide (GO) in deionized water. At -30 °C temperature, this ink was subsequently printed on a current collector made of porous nickel foam. After the droplets containing ATM/GO were frozen, a continuous matrix was produced to form ice crystals. Subsequently, the precursor aerogel was thermally annealed at 600 C for 2 hours to produce a hybrid aerogel of MOS_2-reduced graphene oxide (MoS_2-rGO). SEM imaging of the printed hybrid aerogel revealed the presence of micrometer-sized pores within developed rGO flakes, distinguishing it from traditionally 3D-printed materials. Experimental testing demonstrated reasonable electrical energy storage capacity in the Na-ion battery utilizing the hybrid MoS_2/rGO aerogel anodes, achieving a specific capacity of 800 mAh g^{-1} in the initial cycle at a current density of 100 mA g^{-1}. However, due to the irreversible conversion of MoS2 to Mo and the reversible insertion of two Na+ ions, the specific capacity dropped drastically to 429 mAh g-1 within the first ten cycles. Notably, as the current density increased, the conversion response was less pronounced in the subsequent cycles, resulting in improved stability. In recent years, graphene-based and activated carbon (AC)-based inks are mainly used for developing electrodes for capacitors and micro-supercapacitors, which would be discussed in detail in later sections[64].

Similar to DIW, MXene-based inks are also being explored recently for the generation of flexible electronics products. Wen et al. created MXene/manganese dioxide (MnO_2) hybrid electrodes for wearable ESDs in 2021, which were inexpensive, flexible, and high-performing[65]. The composite was made by inkjet printing with MXene/MnO2 ink, which improved the composite's overall electrochemical performance by allowing rapid transfer of electrons and reduced diffusion routes. The IJP-based composite electrode was tested with a 3400 S m^{-1} conductivity, a high volumetric capacitance of 312 F cm^{-3}, and maintaining 130.8% of its initial capacitance after 500 charging/discharging cycles[65].

In summary, the IJP technique is appealing as an AM method because of its high-resolution output, versatility in generating diverse geometries and designs based on STL files created in CAD, ability to minimize material waste, and ability to print on large areas [66]. Given these overall advantages, there is enormous potential for precisely modifying electrode topologies and boosting the areal energy density of EESDs. The narrow range of printable inks, on the other hand, is a significant issue, as low viscosity is essential for good flowability and successful ejection from printer nozzles. Furthermore, the use of IJP for creating thick electrodes is limited due to the thin layers produced and the relatively slow printing speed[61].

3.1.3. Fused Deposition Modelling (FDM)-based batteries

FDM, also known popularly as 'Fused Filament Fabrication (FFF)', is another material extrusion based AM technique, patented and developed by Scott Crump in 1989, who subsequently founded the first commercial FDM 3D printing company, Stratasys. The process mainly involves 3D-printing by extruding thermoplastic polymers. The polymers are introduced into the extrusion print head in the form of slender filaments, typically with diameters of 1.75 mm and 3 mm, originating from a spool. The extruder is then heated to an appropriate temperature based on the particular polymer employed, surpassing the melting point for semicrystalline polymers or exceeding the glass transition temperature for amorphous polymers[67]. Although the commercialization of FDM has improved its ability to produce a plethora of materials, including polyurethanes, thermosets,

silicones, polymer latex, biomaterials, organic and inorganic pastes, etc., FDM is still restricted to the extrusion of thermoplastics at high temperatures.

Acrylonitrile-butadiene-styrene (ABS) and PLA are the most popular materials used for FDM filaments. More often, these materials are combined with graphene, carbon black, LTO and LFP to increase their electrical conductivity. Hamzah et al. conducted electrochemical characterization of FDM-based ABS/carbon black electrodes for electroanalytical applications and further concluded that the electrochemical behavior of the electrodes was influenced by the printing direction [68]. The printing was done both horizontally and vertically, resulting in a vertically printed electrode (VP) and a horizontal printed electrode with a smooth surface (HPSS) and a horizontal printed electrode with a rougher surface (HPRS) as shown in Figure 4.(a). The smooth surface was generated due to the fact that the first layer of FDM process is thinner than the main layer. The authors found that the VP electrode showed better current response than the horizontally printed electrodes, regardless of the sensitivity of the redox couple. Also, in previous studies it was found that the resistivity in the vertical direction of printing is lower than in the horizontal direction of printing, a consequence of the anisotropy in between the printed layers of ABS/carbon black FDM-based composite electrodes [68,69]. VP electrode was also found to possess the lowest interfacial charge-transfer resistance among the three types of electrodes, indicating that it is more favorable for electron transfer [68]. Furthermore, no appreciable differences in capacitance between the printed electrodes were observed, indicating that the electrochemically active surface remained constant despite variations in surface roughness (Figure 4.(b)). The improved performance of the VP electrodes is due to material's internal structure. This is because the print layers were aligned to match the traces and connect the electrical connection to the solution interface[68].

Compared to ABS, PLA is a better raw material for fabricating composite filaments for FDM filaments as a model fabricated with PLA filaments has poor dimensional accuracy and surface roughness as compared to its ABS counterpart [70]. In early 2022, Ghosh et al. fabricated a photo-electrocatalytically active filament for FDM-based energy storage applications by infiltrating the optimized carbon (mostly activated-carbon and multi-walled carbon nanotubes (MWCNTs) /PLA filament with an active material like MoS_2. The filament fabrication was carried out in two steps: casting of a film of about 2mm thickness and feeding of small pieces of the casted film into the extruder as shown in Figure 4. (d). The AM-based electrode showcased exceptional photoactivity encompassing the entire visible spectrum, displaying the highest activity in the red wavelength range (~600 nm). Moreover, the electrode exhibited an areal capacitance of 381 mF cm^{-2} when subjected to a current density of 1.82 mA cm^{-2}. Impressively, even after undergoing 6000 cycles, the electrode maintained 92% of its initial capacitance (Figure 4. (e))[71].

With commercialization of FDM over the past few years, AM has been utilized for the fabrication of integrated product designs, eliminating the need to manufacture each part separately. As an illustrative instance, the work by Reyes et al. marked a pioneering effort in the advancement of fully-printed and personalized LIBs using FDM 3D printing, customized for specific product design requirements (Figure 4.(c)). Additionally, they performed comprehensive testing on a set of 9 types of carbonate solvents and 3 commonly utilized electrolytes found in commercial LIBs. Their efforts resulted in a significant enhancement of PLA's ionic conductivity to 0.085 mS cm^{-1} and good charge-discharge efficiency (Figure 4.(f)), a fourfold improvement compared to previously reported values. Notably, they successfully fabricated a complete additively manufactured battery cell, encompassing anodes, cathodes, separators, current collectors, and cases. To showcase the versatility of AM, they also integrated these fully printed batteries into a LED bangle and a pair of liquid crystal display (LCD) sunglasses, demonstrating the potential of AM for producing personalized wearable electronic devices [36].

Though FDM is a widely accepted technique worldwide, it does have certain limitations with respect to AM of EESDs. Unlike other methods, FDM requires that the thermoplastics and electrochemical active components be combined before being extruded to

create a filament that can then be used for printing. The time needed for manufacturing as well as the process' overall complexity are both greatly increased. Additionally, a high temperature must be reached for the thermoplastic filaments to reach their glass transition state. A further demerit of FDM printing is that its resolution is typically low particularly along the Z-axis, falling between 50 and 200 um. These limitations can hamper the accuracy and control of the printing process [5,26].

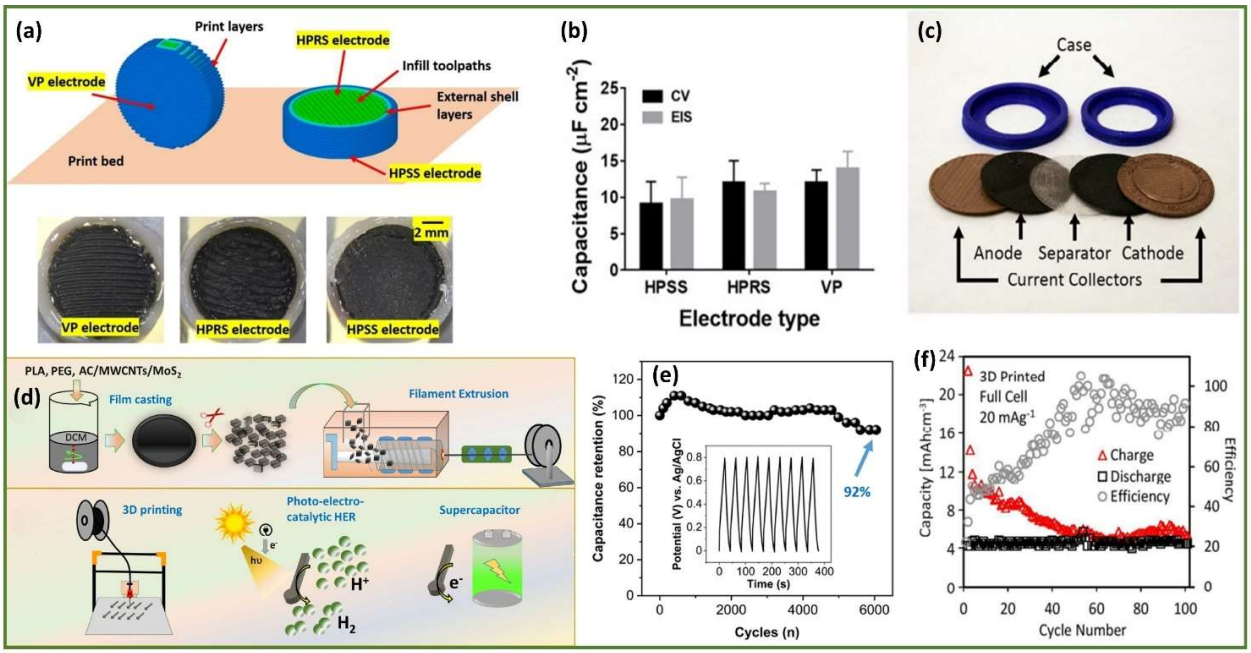

Figure 4: FDM-based batteries and their performances. **(a)** Printing approach and cross-section of the VP, HPSS and HPRS electrodes. **(b)** Capacitance when normalized to the 3D-printed electrode surface area. Reprinted with permission from Hamzah et al. [68] Copyright © 2018, Springer Nature Ltd. **(c)** Current collectors and electrodes printed using FDM, **(f)** Capacity and columbic efficiency of 3D-printed coin cell for 100 cycles. Reprinted with permission from Reyes et al. [36] Copyright © 2018 American Chemical Society **(d)** Filament fabrication schematic of AM-based electrodes in PEC hydrogen evolution reaction and in a supercapacitor **(e)** cyclic stability results for 6000 cycles, inset: charge-discharge cycles for initial 10 cycles. Reprinted with permission from Ghosh et al. [71] Copyright © 2022, Elsevier B.V.

3.1.4. Stereolithography Apparatus (SLA)-based batteries

SLA is the oldest AM technology to be commercialized. Stereolithography operates by selectively curing a photopolymer (resin) using a UV laser. Within the build space of the machine, a slender liquid resin layer, typically with a depth ranging from 50 to 100 microns, is prepared. Utilizing a laser, the desired pattern is precisely sculpted on this layer, selectively curing solely the intended shape within the initial layer of the model. Upon completion of a layer, a fresh layer of liquid resin is generated either by raising the part or lowering the bottom of the build space, thereby facilitating the continuation of the process. Generally, UV curable resins, predominantly based on epoxy or acrylic, and occasionally on vinyl, are utilized in SLA. These resins are initially in a liquid state but solidify upon exposure to UV light. While the early stages of SLA primarily employed a limited selection of low-performance resins, there are now abundant high-performance materials available with diverse characteristics. Although the principle behind Digital Light Processing (DLP) technology and SLA is identical, DLP allows the entire part to be solidified in one pass using optical devices that act as a projector [72].

Similar to the bespoke AM techniques, SLA/DLP also uses active materials like LTO, LFP, graphene, and other 2D nanomaterials as active materials, considering that polymer

resins alone are non-conductive in nature. Cohen et al. used SLA to fabricate porous polymeric substrates in cubic, spherical and cylindrical shapes with high surface areas. These substrates were integrated using an electrophoretic deposition (EPD) process, forming a three-layer structure consisting of a polyethylene oxide (PEO)-$LiAlO_2$ or $Li_{1.5}Al_{0.5}Ge_{1.5}P_3O_{12}$ (LAGP)-polyethyleneimine (PEI) membrane and an LTO anode and an LFP cathode on conductive graphene-filled substrates (Figure 5.(g),(h)). The resulting cell with porous polymer substrate showed a satisfactory cyclic stability performance and reached a surface discharge capacity of 400–500 Ah cm^{-2}.Increasing the cathode thickness and substrate surface area could further enhance these values, in turn, resulting in excellent electrochemical performance. Figure 5.(i) compares the energy density of electrodes printed on different substrates [73].

In recent years, there has been a rise in using recycled wastes feedstock for fabrication of EESDs with increase in sustainability concerns in every manufacturing process. In 2022, Li et al. fabricated a metal-based 3D thick electrode with $NiCo_2S_4$ loading of 18.38 $mgcm^{-2}$ (the active material mass loading increased with electrode thickness) and an areal capacitance of 7.327 mAh cm^{-2} at 44.85 $mAcm^{-2}$, using the DLP process (Figure 5. (a)) [74]. The design approach to manufacture thick electrodes is based on the principle that thicker electrodes increase the active material loading to improve the device energy density. The precursor used for the DLP process are easily recyclable and cost-effective metal salts, subsequently reduced and processed by mild chemicals (acid/salt assisted reaction). The resin utilized in the DLP method in this study consisted of a blend of 1,6-hexanediol diacrylate (HDDA), $M_x(SO_4)_y$ precursor powder, and other active polymers[74].The recycling process for 3D porous metal substrates involved immersing the metal parts in a diluted acid/salt solution. After completing the reaction, the solution underwent filtration to eliminate impurities. The resulting solution was then heated to 90°C until complete evaporation of water, yielding a powder. This collected powder was then subjected to dehydration. In order to ensure the recyclability of the 3D metal porous substrate, the metal salt powder obtained from the above steps was repeatedly used as the feed powder. A specific ratio of dispersant, photoinitiator, and monomer was added to the powder, and after thorough grinding and stirring, a recyclable photocurable resin was developed. The first step involved fabricating the 3D F-KS structure (Figure 5.(b)), which represents an optimized topology highly compatible with DLP printing. The resulting structure underwent post-processing through subsequent heat treatments. Interconnected porosities present at the microscale were observed in high magnification SEM images, demonstrating the sintering of metal particles embedded in the polymer matrix. This process led to a substantial increase in compressive strength for the AM-based nickel substrate compared to commercially available nickel foams, with the 3D-nickel substrate exhibiting nearly 32 times higher compressive strength (Figure 5.(c)). The hierarchical porosity observed in the SEM images contributed to an augmented specific surface area, enabling shorter pathways for ion diffusion, electron transport, and enhanced electrolyte accessibility [71].

Due to slow throughput and limited tool-path, projection micro-stereolithography (PμSL) has been accepted as a popular technique for developing stretchable electronic devices and thin-optimized electrodes. Earlier this year, Batista et al. used a commercial UV-curable resin PR-48 for the fabrication of electrodes via the PμSL process, which was pyrolyzed to obtain the final electrode structure[75]. To enhance the performance, the authors formulated a resin combining 3 wt.% graphene oxide (GO) and trimethylolpropane triacrylate (TMPTA). The topology optimized electrodes showed a 77% gain in capacitance and exhibited better gravimetric capacitance of ~50% capacitance retention at 10 mA cm^{-2} [75].

In conclusion, SLA offers a remarkable opportunity for the efficient fabrication of intricate 3D microlattices. When combined with nanoscale coating and post-processing techniques, SLA can be used to fabricate ultralight and ultrastiff microlattices made of metallic and ceramic materials [61]. Furthermore, the cost-effectiveness and straightforward nature of the SLA process position it as a highly promising high-resolution 3D

printing method with broad application potential across various fields. Despite its numerous advantages, SLA does have some drawbacks. The process is primarily compatible with UV-curable resins, which may restrict the range of available materials compared to other AM techniques. The additional post-processing steps, sometimes, adds to the production cost of EESDs. Moreover, it is generally more suitable for producing intricate objects due to limitations in printing speed and build volume, thus limiting its scalability[72].

3.1.5. Selective Laser Melting (SLM)-based batteries

SLM (also known as Selective Laser Sintering (SLS)), is a cutting-edge powder bed fusion AM technique that utilizes a laser focused as the energy source to selectively fuse metal powder layers, enabling the creation of intricate 3D prototypes [6]. Interestingly, SLM offers the unique advantage of being compatible with a plethora of thermally fusible powder materials, including metals, polymers, and ceramics, without the need for post-processing or complex material processing, as was the case for SLA discussed in the preceding section. These remarkable benefits position SLM as an exceptional technique for precisely fabricating intricate and delicate structures, particularly for applications in manufacturing of EESDs.

Compared to other slurry-based AM processes, SLS enables eliminates the need of solvents or binders during processing, in turn, enhancing the active material loading. AM-based cathodes of lithium nickel cobalt aluminum oxide (NCA- $LiNi_{0.80}Co_{0.15}Al_{0.05}O_2$) were produced using SLS (Figure 5.(d)) with commercially available NCA powder, which had particle sizes ranging from approximately 40 to 300 μm. The received NCA powder consisted of fine primary particles having average diameter of ~0.52 μm and larger secondary particles having average diameter of ~125 μm. The volumetric energy density (VED), representing the amount of energy applied per unit volume of material, was determined for the SLS process using the formula: $VED = P_{eff}/(v\sigma t)$, where v denotes the laser scanning speed, P_{eff} represents the effective laser power, t represents the thickness of the powder bed, and σ represents the diameter of the laser beam. The photograph of the 3D NCA-D50 sample as can be seen from Figure 5.(e) (SLS-produced 3D printed sample with a VED of 50 J mm^{-3}) revealed surface porosity present on the sample top. Additionally, the SEM micrograph exhibited internal porous structures, including gaseous pores and very few fusion pores is also observed in Figure 5.(f). Microstructural analysis of the sample unveiled that the grains closest to the substrate exhibited the finest size, with grain size gradually increasing with height, resulting in the largest grain size at the top of the sample. The microstructure, formation of heterogeneous phase states (due to phase transformation from ordered rock salt (oRS) to disordered rock salt structure (dRS)), and the occurrence of defects and variations in chemical composition within the fabricated 3D NCA samples are attributed to the thermal gradient that develops during the SLS process[76]. This thermal gradient can be attributed to the fact that during the layer-by-layer deposition process in SLS, there is a build-up of thermal energy due to limited heat dissipation caused by the smaller volume of the deposited material. This leads to reduced effectiveness of thermal conduction, as heat flow to the substrate is restricted. Consequently, the cooling rate decreases with increase in build height. As a result, the laser-matter interaction zone temperature rises even with the same amount of input energy per unit length. This reduction in cooling rate promotes grain growth as the interaction zone is subjected to elevated temperatures for an extended duration. Though the fabricated samples did not have higher discharge capacity than the as-received samples due to the formation of dRS phases which was observed to degrade the electrochemical performance, the porous surface and formation of electrochemically active layered structure acts as a foundation for further research into development of 3D cathodes for LIBs [76].

Various approaches are employed in the manufacturing of components for metallic EESDs using powder bed fusion techniques. One such approach involves the printing of a conductive metal substrate using SLM, after which electrochemical deposition of conductive polymers or metal oxides onto the printed electrodes was done to enhance their

electrochemical properties [77]. Additionally, an efficient method for creating carbon scaffolds with high porosity that can be utilized for electrodes is laser carbonization of polymers or polymer-metal composites. The incorporation of metals into the composites improves their mechanical strength and electrical conductivity[78]. Notably, the feedstock powders can be directly sintered or melted to act as current collectors. However, despite its capabilities to work with multiple materials, powder bed fusion techniques still have certain limitations, such as high cost and inherent surface roughness, generation of defects and residual stresses due to thermal gradient, which leave room for further exploration and improvement.

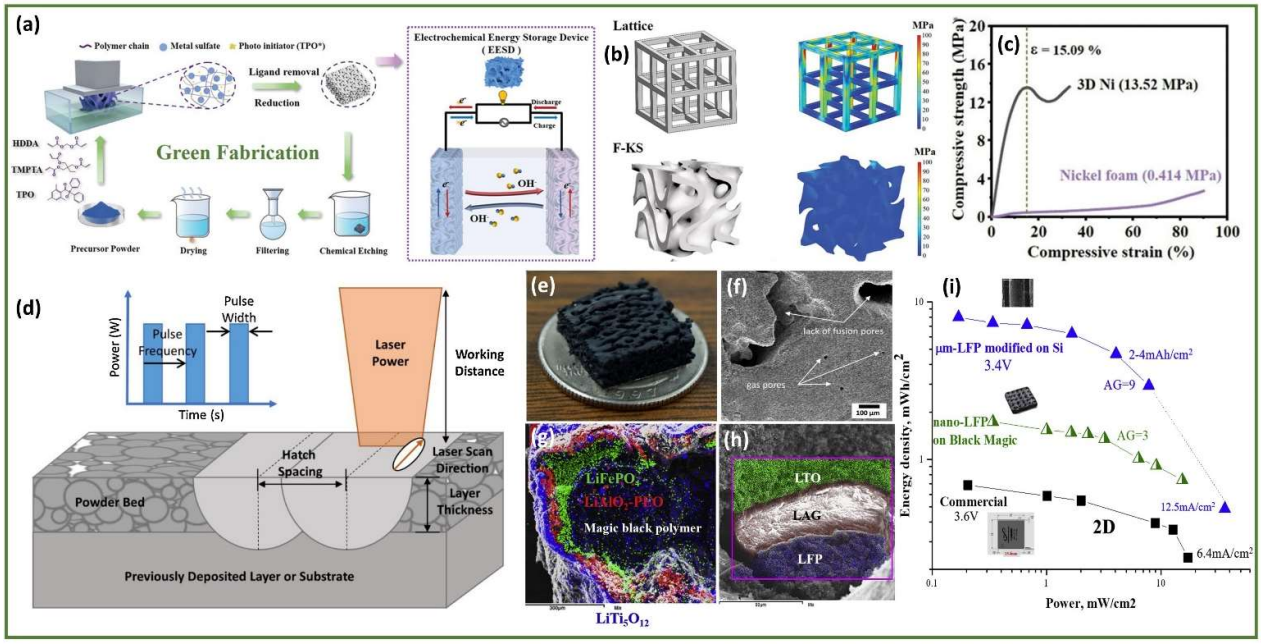

Figure 5: SLA and SLM-based batteries with their respective performances. **(a)** Schematic illustration of stereolithography of 3D-printed sustainable electrodes for nickel iron battery **(b)** FEA models of lattice and F-KS structures of same volumetric density **(c)** Compressive strength of 3DNi and commercial nickel foams. Reprinted with permission from Li et al. [74] Copyright © 2022 John Wiley & Sons, Inc. **(d)** Schematic illustration of SLS process **(e)** Photograph and **(f)** SEM micrograph of a 3DNCA-D50 sample revealing surface and internal porosities. Reprinted with permission from Acord et al. [76] Copyright © 2020 Elsevier B.V. **(g), (h)** Cross-sectional EDS mapping of tri-layer battery structures **(i)** Ragone plot containing electrochemical performance of commercial LIB on graphene polymer substrates, on perforated silicon and on-Black Magic 3D. Reprinted with permission from Cohen et al. [73] Copyright © 2018, Elsevier B.V.

3.1.6. Laminated Object Manufacturing (LOM)-based batteries

Laminated Object Manufacturing (LOM) was patented by Di Matteo in 1974, and was commercialized by California-based Helisys Inc. (at present Cubic Technologies). Layered materials are continuously provided over a platform using a roll and are subsequently cut by means of a laser or knife. An adhesive layer coats these materials, and through the heating of the feeding roller, the adhesive melts, facilitating the lamination process with the previous layer and resulting in the creation of a 3D object. This printing setup offers several advantages, including simplified material handling through continuous sheet feeding and the utilization of efficient laser cutting techniques. These techniques enhance printing speed and achieve a resolution that is competitive when compared to other printing methods [6],[77] Commonly used feedstock materials in LOM includes metals, polymers, or ceramic sheets, which are bonded together using adhesives. Various lamination methods are employed in this technique, such as bonding metal-based sheets, reinforcing

metals or polymers with fibers during lamination, or casting mixed tapes consisting the aforementioned materials[4].

LOM for EESDs is not a well-researched field with the first work being done in 2018 by a group of researchers from Rice University. They synthesized 3D graphene foams (GFs) using LOM, and further refined the structure to form complex 3D shapes with a fiber laser(Figure 6.(a)). To fabricate the laser-induced graphene foams (LIG), the layers of polyimide (PI) were exposed to irradiation. Ethylene glycol (EG) was then applied as a coating to the layers in a stacked fashion. EG, a commonly used binding agent in LOM processes, was considered due to its ability to easily wet the LIG layer, the wetting efficiency being dependent on the specific amount of LIG per unit area. EG acts as an adhesive, facilitating the bonding between the layers through capillary forces, and also provides thermal protection to the LIG during the laser post-processing. The stacked layers, were then subjected to laser fusion, effectively merging the LIG sheets. This sequential process was repeated to construct foams composed of LIG. The LOM-based 3D LIGs were further used as Li-ion capacitor electrodes. Since the self-standing foams exhibit excellent electrical conductivity, binders or current collectors were unnecessary. The electrode materials' performance was initially assessed in half cells, with lithium foil used as both the reference and counter electrode. The anode exhibited an average gravimetric capacity of 354 mAh g^{-1} in the initial 3 cycles. The LIG foam cathode demonstrated 83 mAh g^{-1} average capacity, which is more than the capacity of activated carbon (30-70 mAh g^{-1}). To assemble the complete Li-ion capacitor cell, a mass ratio of 1:5 between the anode and cathode was employed, which exhibited good cyclic stability as observed in Figure 6.(b)[35].

Though graphene sheets have been mainly utilized for LOM-based EESDs, porous ceramics developed recently via this technique is also a viable option for energy storage applications. It has been used in conjunction with freeze casting which is illustrated in Figure 6.(d) to produce porous ceramics. The process involves supplying a slurry and using a doctor blade to scrape it. A cryo-panel equipped with internal refrigerant circulation is employed to freeze the layered slurry. The contour of the frozen slurry layer is then cut and gasified using a laser beam, resulting in the formation of the object's cross-section. Once the printing of the component is completed, it undergoes freeze drying. The compressive strength of the freeze-casted alumina parts is seen to increase with solid content in the slurry in Figure 6.(c) [79].

LOM has not yet been explored, as compare to other AM processes, due to the following disadvantages: (1) The laminated nature of LOM can result in weaker mechanical properties as compared to solid objects. The bonding between layers may not be as strong, leading to reduced structural integrity. (2) Compared to other AM processes, it can be more expensive due to the need for specialized equipment, materials, and adhesive consumables. Moreover, the simple machine design limits accuracy of the manufactured part. (3) Post-processing steps like decubing, finishing and sealing the parts require considerable amount of effort and time [80].

3.1.7. Binder Jetting (BJ)-based batteries

The Binder Jetting (BJ) technology was originally developed at MIT in 1990s. However, owing to the slow progress in this research field, it could only be commercialized in 2010. The printing process can be described as follows: Initially, the print head dispenses binder onto the loose powders based on the desired layer profile. Once a layer is completed, the layer is exposed to an electrical heater to dry the binder-rich areas. Subsequently, the print bed is lowered by a thickness equivalent to one layer while the feed bed is raised. A roller then uniformly spreads a new layer of powder onto the previously printed layer. This layer-by-layer process continues until the entire object is successfully constructed[81]. The BJ fabrication process mainly involves two materials: powders which can be metal, polymer, or ceramic, and the binders.

Several factors related to the powder and binders significantly influence the printing process and the final quality of the parts produced. The size and shape of powders play a

crucial role. Finer powders offer advantages such as higher resolution, reduced surface roughness, and improved post-processing sinterability. However, fine powder particles tend to clump together during deposition, resulting in poor flowability. Therefore, powders having an average particle size greater than 20 um are usually recommended. Additionally, spherical particles are preferred due to their superior flowability, owing to less friction between particles and layers. The thickness of the deposited powder layers, which is influenced by the slicing procedure and powder properties, is another crucial factor to take into account. Although a thinner layer extends the manufacturing process, it can improve model resolution. However, extremely thin layers can lead to excessive binder penetration, resulting in unwanted spreading to neighboring areas and negatively affecting resolution and tolerance. On contrary, thicker layers require higher binder saturation[82].

The only work reported till now regarding BJ for EESDs is that done by Azhari et al. in 2017. In their study, the authors used BJ for the production of graphene-based electrodes, mainly for supercapacitors and not batteries. As of now, there has been no work on complete cell fabrication using BJ technique. For the fabrication process, thermally reduced graphene oxide (TrGO) powders were procured from graphite through exfoliation and thermal reduction. The TrGO powders were mixed with acetone and dried through evaporation to improve their flowability. Following the evaporation process, the TRGO is utilized to construct electrodes with desired shapes and thicknesses through a layer-by-layer buildup method using optimum amount of binder. These electrodes exhibit remarkable capacitances of 260 F g^{-1} and areal capacitances of 700 mF cm^{-2} in a 1m H_2SO_4 electrolyte when directly employed in supercapacitors. Moreover, to optimize the performance, a small quantity of palladium nanoparticles was introduced into the printed electrodes to enhance the contact resistance among the agglomerated powder particles[34].

Additional post-processing treatments and expensive equipment add to the overall production cost of BJ-based materials. This area is one of the least explored AM processes for not only EESDs but also structural parts as the materials formed are usually brittle. Extensive research is still required in this field to optimize the binder-jetting process to make it more economical.

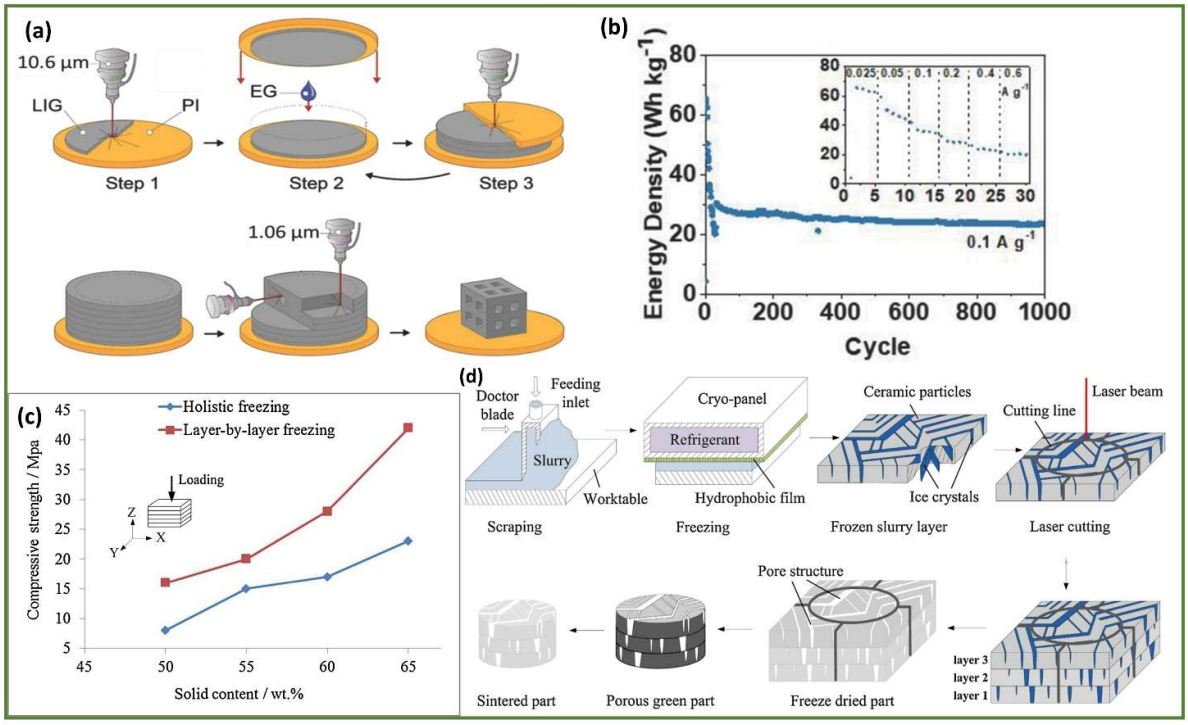

823

Fig 6: LOM-based batteries and their performances. **(a)** Schematic of the LOM and fiber laser milling process **(b)** Cyclic stability of 3D LIG Li-ion capacitors. Reprinted with permission from Luong et al. [35] Copyright © 2018 John Wiley & Sons, Inc. **(c)** Comparing compressive strength of porous alumina parts by layer-by-layer and holistic freezing **(d)** Schematic illustration of frozen slurry based-LOM process. Reprinted with permission from Zhang et al. [83] Copyright © 2018 Elsevier Ltd.

3.2. Additive Manufacturing of capacitors and supercapacitors

In the previous section, we mentioned different additive manufacturing techniques for batteries by highlighting the pros and cons of every process, and citing few examples or works based on the application of the process being discussed in the manufacturing of batteries or electrodes.

A capacitor is a passive electronic component, that can be fully additively manufactured by first printing the bottom electrode on the substrate, which is followed by printing of dielectric material and the top layer. In the printing process, it is necessary to sinter the bottom conductive layer before proceeding to print the dielectric and top conductive layers[84].

In case of supercapacitors, which can be considered as a hybrid of high energy density batteries and high power density capacitors, the main components are the electrodes and electrolyte. The typical materials used for fabrication of electrodes are metal oxides, carbon-based materials like CNFs, graphene and its derivatives, and metal oxide frameworks (MOFs), and conducting polymers. Supercapacitor electrolytes can either be liquid, solid or redox-active[85]. The AM processes employed for capacitors and supercapacitors are similar to that for batteries, but differ with respect to materials used, designs, and post-processing of the fabricated parts.

In this section, we would delve into AM of another class of EESDs: capacitors and supercapacitors, mainly focusing on the research done in this area as the individual AM processes have already been explained in Section 3.1.

3.2.1. DIW-based supercapacitors

Similar to AM batteries, inks based carbon-based materials are popularly used for the fabrication of supercapacitor electrodes by the DIW process due to their chemical stability, high specific surface area (necessary to facilitate ion-transport) and mechanical strength. For example, a novel gel ink containing polyaniline (PANI) and GO developed successfully through self-assembly in a blend solvent was used for DIW-printing of electrodes. The fabrication process is illustrated in Figure 7.(a) and the 3D-printed lattice structure is shown in Figure 7.(b). The developed ink demonstrated excellent shape retention and extrusion properties due to its optimum modulus and viscosity. The authors were successful in printing a variety of complex architectures, such as 3D honeycombs, hollow thin-wall columns and column lattices, with high resolution and structural integrity. When subjected to higher current densities, the specific capacitance of the printed electrodes reduced to 342±5 F g^{-1}, reaching 81% of its value at lower current densities as shown in Figure 7.(e). The CV curve in Figure 7.(d) also demonstrates the excellent electrochemical performance of the fabricated electrodes. Additionally, the all-printed planar solid-state supercapacitor exhibited an exceptional 1329 mF cm^{-2} areal specific capacitance at 4.2±0.8 mA cm^{-2}, which represents the highest achievement to date using the DIW method[85,86]. Similarly, Chen and co-workers used carbon nanotube (CNT)-based ink for the fabrication of fully-packaged supercapacitors. In this work, fully packaged and sealed supercapacitors were fabricated directly on a flexible polyimide substrate using a CNT ink consisting of single-walled carbon nanotubes (SWCNTs) as a major component, with a silicone packaging and PVA gel electrolyte . By experimenting with different cell configurations, it was determined that altering the width of the electrode patterns and reducing the distance between electrodes could significantly improve the printed supercapacitor's capacitance. The specific capacitance of the produced array of supercapacitors reached its peak at 15.34 F cm^{-3} when subjected to a current density of 1.32 A cm^{-3}.

Additionally, the corresponding power and energy density values were measured at 11.8 W cm^{-3} and 1.18 mWh cm^{-3} and, respectively. Notably, the supercapacitors exhibited excellent cyclic stability, retaining 96.5% of their capacitance after undergoing 5000 charge/discharge cycles at 1.32 A cm^{-3} current density[61,87].

Metal oxides and noble metals are also widely explored as active materials for micro-supercapacitors due to their significant pseudocapacitive capacitance. However, these materials are prone to structural collapse over long cycles. This issue can be addressed by incorporating other active materials, which serve as mechanical support and provide the required electrical conductivity. In 2011, Guo and his research team pioneered the use of Zinc oxide (ZnO) as flexible supercapacitor electrodes. They developed a flexible supercapacitor electrode by fabricating a sandwich structure of rGO-ZnO nanorods-rGO through chemical vapor deposition (CVD) on a graphene film-polyethylene terephthalate substrate[88]. In 2017, a novel asymmetric fibered supercapacitor (AFS) was developed using active carbon fiber (ACF) as the negative electrode and cobalt oxide-polypyrrole (Co_3O_4-ppy) core-shell nanorod arrays as the positive electrode (Figure 7.(b)). The Co_3O_4-ppy core-shell nanorods exhibited high capacitance due to their excellent redox properties, while the ACF provided stability and reliability. The AFS showed excellent supercapacitive performance with 1.151 mWh cm^2 energy density and 1.15 mWcm^2 power density. It also showed remarkable cyclic stability and excellent durability during bending tests. These exceptional electrochemical and flexible properties (Figure 7.(i))also make it promising for developing flexible wearable micro-energy storage devices[89].

MXene-based inks are a commonplace for not only batteries but also for supercapacitors due to their bespoke properties. For example, Orangi et al. developed all-solid-state MSCs by using a water-based MXene ink (Figure 7.(g),(h)). The 2D $Ti_3C_2T_x$ based ink used for the DIW printing has outstanding electrochemical properties, hydrophilicity and high electrical conductivity, making it an ideal material to be used for 3D-printed EESDs. Initially, $Ti_3C_2T_x$ was prepared by etching Al atoms from Ti_3AlC_2 MAX phase particles dispersed in an aqueous mixture of LiF and HCl, followed by dispersion of the produced $Ti_3C_2T_x$ ink in DI water and sonication to produce delaminated MXene flakes. The prepared ink demonstrated rheological properties that fitted the Hershel-Bulkley model (Section 3.1.1). MSCs with different electrode thickness were prepared by first printing the current collectors, and then printing the subsequent layers on the finger region of the printed patterns as shown in the figure. The power density and areal energy density were calculated to be 3.7 mW cm^{-2} and 8.4 μW h cm^{-2} respectively and good electrochemical properties for a MSC with only 1 printed layer (Figure 7.(f)). The MSC device with 10 printed layers achieved the highest recorded areal energy density of 51.7 μW h cm^{-2} and 5.7 mW cm^{-2} power density. However, due to its improved time constant compared to 1 layered MSC, the power density decreased significantly as the scan rate was increased[90].

Though DIW allows the utilization of a plethora of materials, there is considerable amount of post-processing involved such as drying, annealing, or surface modifications to improve their electrochemical performance. Another issue that is often faced is scaling up DIW production of supercapacitors.

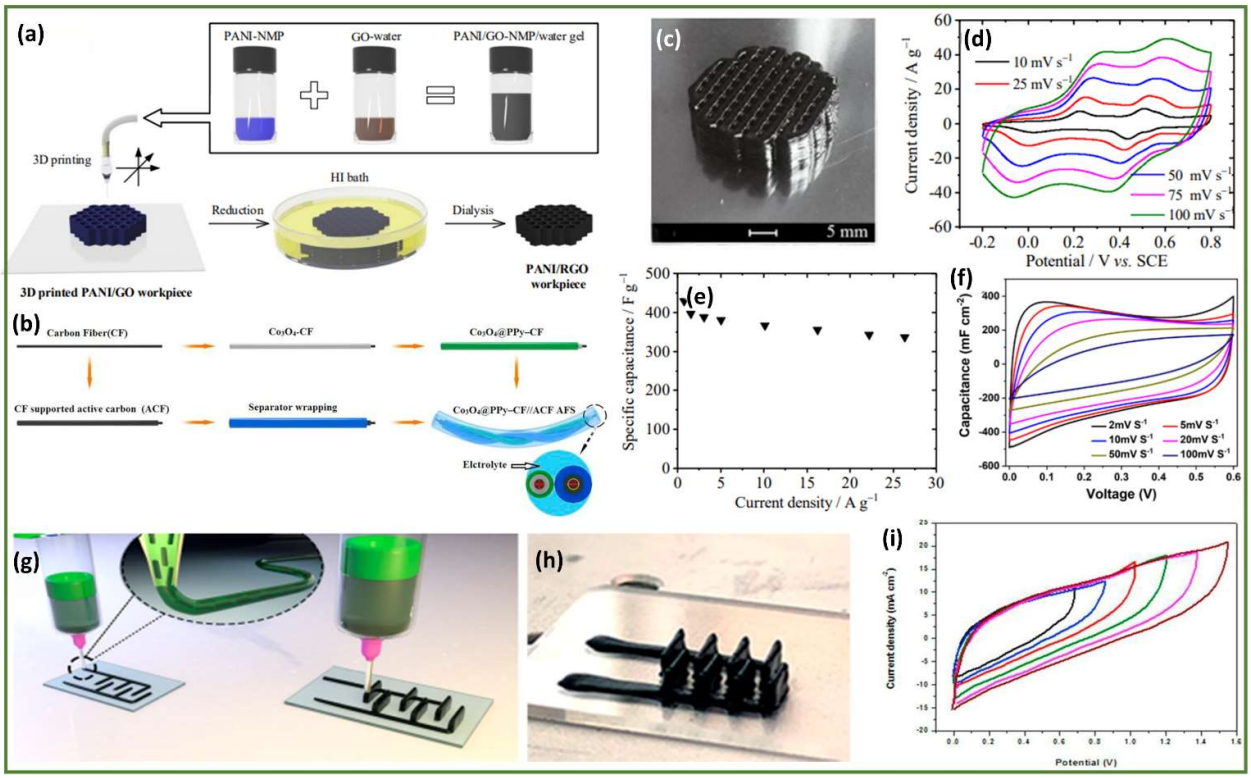

Figure 7: DIW-based capacitors and their performances. **(a)** Preparation of PANI/rGO inks and fabrication of AM-based electrodes **(c)** 3D-printed PANI0.4/GO column lattice structure **(d)** CV curves at different scanning rates **(e)** Specific capacitance at different current densities. Reprinted with permission from Wang et al. [86] Copyright © 2018 American Chemical Society **(b)** Flexible asymmetric-fibered supercapacitor of nanorod arrays **(i)** CV curves at different scan rates. Reprinted with permission from Wu et al. [89] Copyright © 2017 Elsevier B.V. **(g)** Schematic illustration of DIW printing of interdigitated electrodes (h) Optical image of the printed MSC on a glass substrate **(f)** CV curves of MSC printed with 1 layer at various scan rates. Reprinted with permission from Orangi et al. [90] Copyright © 2019 American Chemical Society.

3.2.2. IJP-based supercapacitors

Inkjet Printing (IJP) has been widely utilized in the fabrication of supercapacitors. Li et al. conducted research in this area and developed a flexible supercapacitor with three layers using this technique. The device was constructed by depositing silver nanoparticles (Ag-NPs) and rGO onto a substrate, followed by electrodeposition of Ni-Co Layered Double Hydroxides (LDHs). This unique design eliminated the need for binders and facilitated rapid transfer of electrons due to the presence of Ag-NPs between the two layers. Building upon their previous work, the same team of researchers also developed a multi-layered electrode consisting of Ni-Co LDH and rGO layers. This modification led to improved performance in various aspects while maintaining device stability[91].

Conductive polymers also show immense potential as materials for electrodes of IJP-based supercapacitors because of their high pseudo-capacitance. Among them, PANI is a commonly studied conductive polymer known for its unique electrical and optical properties. However, PANI has certain drawbacks when used as a supercapacitor electrode, such as low mechanical strength, poor cyclic stability and moderate conductivity. Hence, hybrid electrode materials containing an active material is utilized to compensate for the bespoke disadvantages[92]. In a study, a two-electrode symmetric supercapacitor device was developed using a nanographene platelets (NGP)/PANI electrode and H_2SO_4 electrolyte. The NGP and NGP/PANI materials possessed the property of easy dispersion in water, forming thin transparent sheets that are electron-permeable for TEM analysis.

By directly printing the NGP/PANI composite onto a carbon fiber substrate, an electrode can be fabricated without the need for additional processing steps. The two electrodes were then separated by a diaphragm to construct a capacitor. The resultant supercapacitor demonstrated exceptional electrochemical performance and long-lasting cycle stability. This investigation showcases the applicability of IJP in the development of supercapacitors, particularly utilizing the NGP/PANI composite composed of readily available and cost-efficient materials. It lays a practical groundwork for the progress of printable energy storage devices[93].

IJP has also been recently used for printing lightweight supercapacitors on textiles. In the fabrication of electronic textiles (e-textiles), IJP offers several advantages compared to conventional manufacturing techniques[94]. It allows for precise deposition of controlled amounts of materials at specific locations on the fabric, while also reducing material waste and water usage. However, a significant obstacle in IJP for electronic textiles (e-textiles) lies in achieving consistent conductive electrical tracks on porous and rough textile substrates using inkjet inks with low viscosity. To overcome this challenge, Stempien et al. proposed an innovative approach in IJP that involves freezing inks at various temperatures, even as low as -16 °C, to create polypyrrole (PPy) layers on textile fabrics. These PPy-coated layers were then utilized as electrodes on polypropylene (PP) textile substrates, forming a symmetric all-solid-state SC device (SSC). The electrochemical analyses indicated that the device exhibited a maximum specific capacitance of 72.3 F g^{-1} at a current density of 0.6 A g^{-1}. Furthermore, it demonstrated an impressive energy density of 6.12 Wh kg^{-1} and a corresponding power density of 139 W kg^{-1}. To summarize, the proposed IJP method, which involves the direct freezing of inks at sub-zero temperatures, enables the creation of PPy layers on textile fabrics. These PPy-coated fabrics effectively function as symmetric SSC electrodes, showcasing exceptional electrochemical performance characterized by high specific capacitance, energy and power density. This research underscores the potential of IJP in fabricating e-textiles and driving advancements in wearable energy storage devices. [95].

3.2.3. FDM-based supercapacitors

Unlike other manufacturing techniques, FDM has not widely been used for manufacturing supercapacitors. Foo et al. developed a supercapacitor and a photoelectrochemical (PEC) sensor using the FDM technique. Instead of utilizing usual commercial electrode materials like glassy carbon, ITO glass, the authors fabricated the components using a conductive graphene filament. This was accompanied by electrodeposition of Ppy, an electroactive material, on the electrode surface, resulting in a SSC with PVA-KOH electrolyte. Each electrode was printed in the form of an elongated strip, followed by gold sputtering to increase its conductivity. These gold-sputtered electrodes served as current collectors and Ppy/rGO nanocomposites were then deposited on them. After some basic post-processing treatments, these electrodes were pressed into PVA-KOH gel electrolyte to complete the fabrication of the supercapacitor. The specific capacitance was reported to be 98.37 Fg^{-1} at 0.5 Ag^{-1} current density, thrice that of other 3D printed supercapacitors. Though the capacitance retention dropped after 100 cycles, the gold-sputtered electrodes exhibited good cyclic stability over the first 100 cycles. The authors also tested the effect of CdS nanocomposites as an active material, which was doctor-bladed on the gold-sputtered electrodes for developing the PEC sensor. The developed PEC sensor even had an apparently higher photocurrent intensity than other 3D-printed PECs reported earlier[96].

In another recent study by Zhang et al., an industrially replicable and cheap method was introduced with an aim to produce flexible MSCs was introduced, combining FDM printing and stamping techniques using MXene-based ink (I- $Ti_3C_2T_x$). Specifically, FDM-printed stamps were utilized, which could be designed in various shapes such as interdigitated, yin yang, or spiral patterns. These stamps, after coating with 2D MXene inks, were pressed onto substrates like paper, polyethylene terephthalate (PET), or glass, resulting in the formation of MSCs with controlled electrode patterns. The finger-shaped

electrodes of the MSCs showed high uniformity, with specific dimensions (W_g~550 μm, W_e~ 415 μm) and compactly stacked MXene flakes, forming a continuous and conductive film network. This configuration led to the MSCs demonstrating a high areal capacitance of 61 mF cm-2 at 25 μA cm^{-2} current density. Furthermore, the MSCs exhibited good rate capability, with approximately 82% capacitance retention at 800 μA cm^{-2} higher current density. The devices also showed excellent long-term stability, maintaining their perforance over large number of cycles. Additionally, they also displayed exceptional flexibility, as minimal changes in capacitance (less than 20 %) were observed when the devices were bent or twisted. The above two discussed studies highlight the potential of FDM for scalable and rapid production of flexible supercapacitors with promising performance characteristics[97].

3.2.4. SLA-based supercapacitors

SLA has emerged as a promising technique for the fabrication of durable supercapacitors, as demonstrated by recent works. In 2020, Chang et al. utilized SLA to create highly flexible Ni-Co LDH supercapacitors. Notably, these LDHs exhibited a negative Poisson's ratio (NPR), which contributed to exceptional mechanical properties such as impact toughness, improved shear strength, and flexibility. The supercapacitors showcased remarkable flexibility, capable of bending up to 180 degrees, and impressive stretchability of up to 50%. Even after subjecting the supercapacitors to 1000 stress cycles, the capacitance remained at 75.2% of its initial value. Likewise, after undergoing 5000 cycles of 180° bending, the capacitance was preserved at 88.1% of its original value[98].

In an older study in 2016, high dielectric capacitors were fabricated using the projection-based SLA method. The enhancement of dielectric permittivity was achieved by incorporating surface-decorated Ag on $Pb(Zr,Ti)O_3$ (PZT-Ag) particles as fillers. Photocurable polymer solutions were utilized to create polymer nanocomposites.The Flex/PZT-Ag composite exhibited a significantly high dielectric permittivity of 120 at 100 Hz, with an 18 vol% filler content, which is approximately 30 times higher compared to pure Flex. This fabrication approach relied on integrating dielectric particles within a photocurable polymer resin, leveraging this type of SLA process. The notable improvement in dielectric permittivity was achieved by improving the effective poling of PZT particles and the MWS effect through PZT particles surface decoration with Ag coating. Additionally, the composite demonstrated low loss, due to suppression of electric distortion and charge transfer blockage by the polymer resins. The AM-based capacitor's specific capacitance was determined to be around 63 F g^{-1} at 0.5 A g^{-1} current density. CV curves indicated that this particular type of AM-based capacitor exhibited low impedance and excellent capacitive properties. The ability to produce complex 3D architectures with superior capacitive performance makes the capacitor an attractive prospect for prospective applications in high-energy density systems and 3D-printed embedded devices with remarkable charge-storage capabilities[99]. SLA, unlike FDM, offers the advantage of printing in higher resolution and also facilitates the formation of hierarchical porous structures.

SLA is also preferred for its ability to generate a nearly defect-free product and high dimensional control. Carbonaceous materials dominate the SLA process too, resulting in efficient supercapacitors. A recent article presented a simple technique to fabricate complex 3D pyrolytic carbon electrodes via SLA and subsequent pyrolysis. The study focused on optimizing three essential factors: the choice of carbon precursor, the architectural design of the 3D printed structure, and the conditions during pyrolysis, all aimed at achieving well-defined and consistent carbon electrodes. To comprehend the influence of the precursor's degradation rate on the properties of the carbonized structures, two distinct pyrolysis processes, namely rapid and gradual, were implemented. The results revealed that the pyrolysis process had a more significant effect on the samples' electrochemical properties compared to the final pyrolysis temperature, as evaluated within the tested temperature range[100].

3.2.5. SLM-based supercapacitors

SLM, a technique primarily employed for metal alloys, has shown promising results in the manufacturing of supercapacitors. Zhao and colleagues accomplished a successful application of SLM to create a titanium-based supercapacitor. They utilized electrodeposition to deposit Ppy onto a titanium frame, resulting in electrodes that resembled a square comb structure (titanium alloy-teeth, electrodeposited Ppy-electroactive material). Due to its highly porous structure, the device exhibited 2.4 F cm^{-3} capacitance and 213.5 Wh m^{-3} energy density[101]. Similarly, Lu et al.[102] combined electrodeposition with SLM to synthesize a supercapacitor electrode consisting of a PANI-coated Inconel 718 substrate. The coating contributed a Faradaic pseudo-capacitance to the device, resulting in an improved capacitance. 3D-printed stainless steel electrodes with a helical shape were fabricated using SLM process, which serve as platforms for diverse electrochemical devices. This is accomplished by precisely controlling the electrochemical deposition of IrO_2 films onto the electrodes. The recorded current signals clearly indicate a consistent increase, signifying the successive IrO_2 layer deposition on the electrode's surface. In terms of their application as electrochemical capacitors, the fabricated electrode demonstrated a specific capacitance of 14 mF cm^{-2} at a current of 0.1 mA in alkaline medium[103].

3.2.6. AM of electrolyte materials

An electrolyte is a fundamental component of both batteries and supercapacitors, which can be either liquid or solid-state. In the past decade, research on solid-state electrolytes have gained significant momentum due to their inherent advantages. A major advantage of solid-state batteries is their improved safety compared to traditional lithium-ion cells, as they eliminate the need for flammable liquid electrolytes. Inorganic solid electrolytes enable battery operation at extreme temperatures where liquid electrolytes would either decompose, boil or freeze. The low activation energies in solid-state batteries ensure stable ionic conductivity over a wide temperature range. Additionally, solid-state technology has the potential to significantly increase energy density, which is crucial for any efficient energy storage application. However, a notable drawback of solid-state batteries is their dependence on contact between solid particles for ionic diffusion. These point contacts are stress-sensitive during cycling tests, leading to the formation of cracks and delamination of interfaces. Another significant challenge is ensuring the stability of interfaces in solid-state batteries. The composition and structure of the interfaces between solid electrolytes and electrode materials often differ significantly from the bulk materials. This can result in the formation of decomposition products that hinder the performance of solid-state devices by either impeding ion conduction or promoting electron conduction. To better understand and address these issues, researchers have developed various computational and experimental techniques to investigate the formation and behavior of these interfaces[104].

Achieving precise control on porosity in battery membranes is crucial for enhancing their long-term cyclic stability, and inhibiting the formation of dendrites. However, conventional methods face challenges in fabricating high-performance membranes with precisely controlled pore sizes. Recently, Blake et al. introduced a novel approach for 3D printing ceramic-polymer electrolytes (CPEs) that are both flexible and high-performing (Figure 8.(b),(c)). In their study, they dissolved PVDF and glycerol in NMP and combined them with a significant amount of Al_2O_3. Upon drying, the solid liquid-like glycerol and PVDF separated, creating a porous structure. The resulting polymer electrolyte (CPE-PI) exhibited superior wettability compared to commercialized separators, allowing for rapid and complete wetting within 30 minutes. This characteristic is beneficial for streamlining the electrolyte-filling process and extending the battery's lifespan. After the thermal stability tests, Celgard 2325 exhibited continued shrinkage with increasing temperature and CPE-PI demonstrated excellent thermal stability, with only a 3-5% shrinkage at high temperatures. The developed electrodes also exhibited good electrochemical performance (Figure 8.(d))[105].

In a recent study published in 2022, Lee et al. developed the first 3D-printed high-modulus solid polymer electrolyte (SPE) using DLP technique in the shape of Australia (Figure 8.(a),(e)), representing a promising progress in AM of EESDs. The SPEs consisted of a continuous domain of PEO (polyethylene oxide) swelled with BMITFSI (1-butyl-3-methylimidazolium bis(trifluoromethylsulfonyl)imide: an ionic liquid) within a crosslinked matrix of isobornyl acrylate (IboA) / trimethylolproprane triacrylate (TMPTA). These SPEs exhibited exceptional properties, including a high shear modulus ($G' > 108$ Pa) and impressive ionic conductivity (up to $\sigma = 3 \times 10^{-4}$ S cm^{-1}) at room temperature(Figure 8.(i)). With increase in the volume fraction of conductive components, the ionic conductivity significantly improved while shear modulus decreased by a small amount. It is worth noting that all the SPEs produced through this 3D printing technique remained rigid polymeric solids at room temperature[106]. Another study published in the same year used solid-state ionogel, 1-ethyl-3-methylimidazolium bis(trifluoromethyl sulfonyl)imide ([EMI][TFSI]) embedded in PVDF-*co*-hexafluoropropylene (PVDF-HFP)) as electrolytes as they offer high viscosity, large ionic size and broad operating potential range with porous electrodes(Figure 8.(f),(g)). Achieving an appropriate balance between the ionic liquid and polymer is critical when developing an ionogel ink suitable for AM. Insufficient polymer content leads to instability and collapse of the printed gel. On contrary, the ink's polymer concentration enhances the cross-linking, resulting in a self-supporting gel with adequate mechanical strength. In their investigation, they determined that the optimal polymer to ionic liquid ratio for successful AM process was 9.3 wt.%. The resultant 3D printed MSCs displayed exceptional performance, including a remarkably high specific capacitance of 110.4 mF cm^{-2} at a voltage of 2 V. This high capacitance value translated into an impressive 60.6 μWh cm^{-2} energy density. They also maintained 96.2% of initial capacitance after 2000 cycles and demonstrated mechanical stability (Figure 8.(h)) [107]. In addition to the commonly printed quasi-solid electrolytes, there have been reports of solid-state ceramic electrolytes containing Li-ion and separators . Additive manufacturing techniques enable the printing of electrolytes and separators using different raw materials or the addition of diverse fillers, allowing for the fabrication of components with customized thermal, physical, mechanical, and electrochemical properties. This flexibility in material selection and the ability to create components in arbitrary shapes contributes to improved performance in energy storage devices[108].

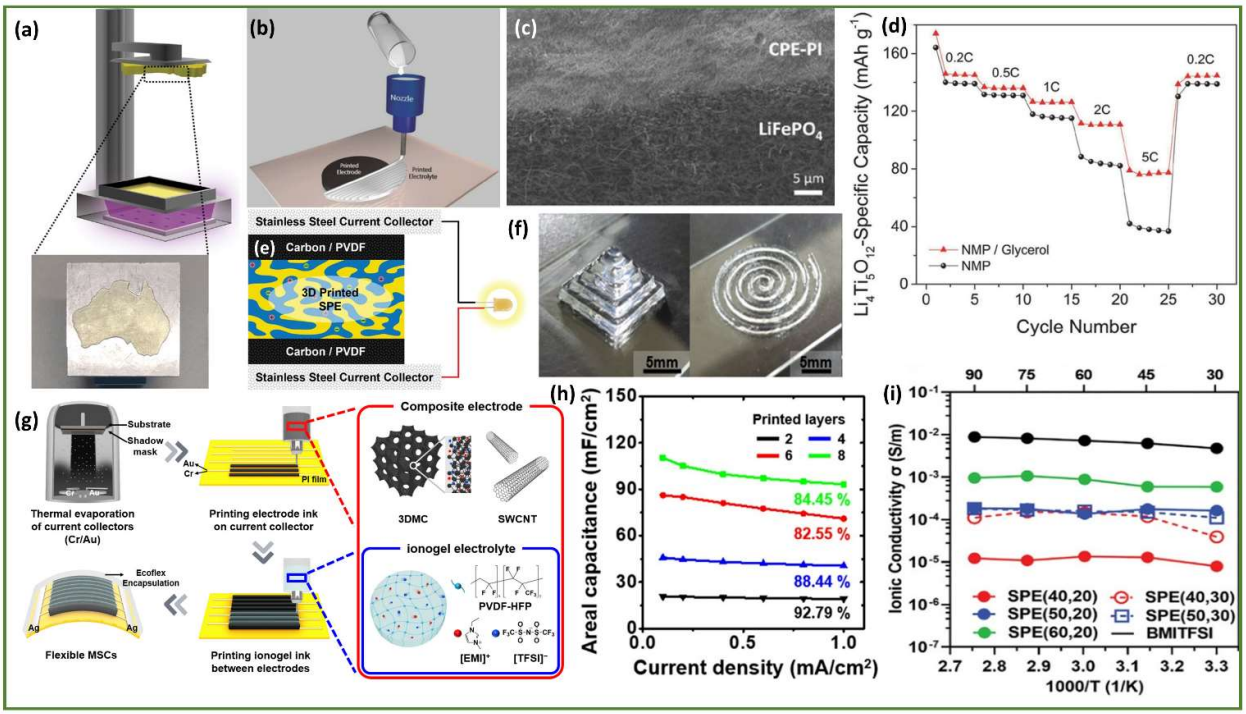

Figure 8: Additive manufacturing of various solid-state electrolyte materials. **(a)** Schematic illustration of the AM process for printing solid polymer electrolytes in the shape of Australia and **(e)** assembled symmetric supercapacitor **(i)** Ionic conductivities of electrolytes with different widths as a function of temperature. Reprinted under Creative Commons CC BY license from Lee et al.[106] Copyright © 2022 John Wiley & Sons, Inc. **(b)** Printing process and **(c)** cross-sectional SEM image of polymer electrode membrane assembly **(d)** Electrochemical rate performance of composite electrodes. Reprinted with permission from Blake et al. [105] Copyright © 2017 John Wiley & Sons, Inc. **(g)** Printing flexible MSC electrodes with printable ionogel electrolytes **(f)** Photographs of printed ionogels with various structures **(h)** MSC capacitance retention with various number of electrode layers. Reprinted with permission from Cho et al. [107] Copyright © 2022 Elsevier B.V.

3.3. Additive Manufacturing of fuel cells

The fundamentals of fuel cells (FCs) have already been discussed in the introduction. This technology can be classified into three primary groups on the basis of the type of electrolyte used: Alkaline Cells (ACs), which rely on alkaline solutions, PEMFCs, which use polymeric materials, and Solid Oxide Fuel Cells (SOFCs), which use ceramic materials. Using AM technologies has a significant potential to benefit from various perspectives given the complexity of fuel cell and electrolysis technologies, which involve intricate systems made up of specialized gas manifolds and multi-layered electrochemical cells[109].

In the following sections, we will delve into these aspects and explore other pertinent factors related to the utilization of AM-based technologies in fuel cell, drawing insights from existing literature. Furthermore, as the field of AM continues to advance, it enables greater flexibility and customization in the design and fabrication of FCs. This, in turn, opens up new possibilities for improving their performance, efficiency, and overall integration with other components. The synthesis of innovative materials, the optimization of cell architecture, and the enhanced functionality of interconnectors and gas management systems are just a few areas where 3D printing techniques can have a transformative impact. By leveraging the capabilities of 3D printing, researchers and engineers are striving to unlock the full potential of fuel cells and electrolysis systems, driving us closer to a sustainable and energy-efficient future.

3.3.1. IJP-based fuel cells

An oxide-ion conducting electrolyte separates the two electrodes in a SOFC. The cathode uses oxygen from the air as the oxidant, whereas the anode permits direct fuel oxidation. The electrolyte plays a critical role in the SOFC, requiring it to be thin and dense. The thickness restricts the fuel and oxidant mixing, while thinner electrolytes minimize ohmic losses and area-specific resistance[109]. Farandos et al. [110]conducted research on fabricating a 23 μm YSZ electrolyte using IJP, optimizing the conditions for anode printing. The SEM cross-section demonstrating all the layers can be seen in Figure 9.(e), along with the principle of drying process in Figure 9.(f).

Improving the performance of the SOFC anode can also be achieved through optimizing the printing conditions. Tomov et al. explored the optimization of a NiO-GDC anode's printing conditions using two different suspensions based on methanol (MeOH) and 1-propanol (PrOH) solvents. The direct ceramic IJP technique, which allows for non-contact dispensing of droplets in nanoliter volumes, was employed. Here, the anode was inkjet printed on a porous stainless steel scaffold[111]. To address other important challenges of sulfur poisoning and carbon deposition in the Direct Carbon SOFC, Dudek et al. [112] utilized an inkjet-printed Ni-YSZ anode infiltrated with a $Cu(NiO_3)_{2.3}H_2O$ solution. This method improved electric conductivity while also preventing sulphur poisoning, corrosion, and carbon deposition. With the infiltration of Cu solution, the performance of the cells increased, reaching 80 $mWcm^{-2}$ at 850°C as opposed to 60 $mWcm^{-2}$ without Cu infiltration. In the case of cathodes also, inkjet printing techniques offer advantages over other methods. Lee et al. found that the IJP-based composite cathode (Fabrication process in Figure 9.(c)) performance surpassed that of an IJP-based single-component cathode. The inkjet-printed Ag-SDC (samarium-doped ceria) composite cathode demonstrated high power and current densities, and lower polarization losses compared to the IJP-based Ag cathode(Figure 9.(d))[113]. Therefore, the use of composite inkjet-printed electrodes should be considered to achieve enhanced electrochemical performance. Overall, the application of IJP in the fabrication of SOFC components, such as electrolytes, anodes, and cathodes, offers opportunities for improved performance, precise control, and advanced functionalities in SOFC systems.

The materials utilized in PEM cells have remained largely unchanged since the early 1990s. PFSA membranes have been the predominant choice for the electrolyte, offering high proton conductivity and chemical stability. These thin and flexible membranes can conduct electricity only when they contain water. In terms of electrodes, platinum on carbon catalysts is commonly employed for both the anode and cathode in PEM cells. These catalysts facilitate the necessary electrochemical reactions within the cell. Flow plates or bipolar plates play a crucial role in PEM cells as they ensure an even air and fuel gas distribution, enable conduction among cells, remove heat generated in the active area, and prevent any leakages[109]. Though traditionally high-density graphite has been used for bipolar plates, there has been a shift towards using metal, moldable graphite, or polymer composites in recent times.

In a recent work by Willert et al. in 2022, the authors used IJP for printing catalyst coated membranes (CCMs), without relying on any intermediate substrates. For multilayer production, three distinct strategies were created and put into use, with varied levels of inkjet printing. In the first way, a foundation layer made of a catalyst layer was coated using a slot-die technique. Then, employing IJP, an ionomer layer and a second catalyst layer were successively coated on top of the first surface. The substrate for the catalyst layer deposition in the second method was a commercial membrane. In the third technique, all three layers were applied via IJP, with an ePTFE film as the initial membrane reinforcement substrate. The entire fabrication process has been illustrated in Figure 9.(a) and the sequence of printed layers are shown in Figure 9.(g). The catalyst and membrane layers obtained were thoroughly analyzed and demonstrated uniformity concerning ionomer distribution, catalyst loading and thickness consistency. The catalyst layers had a catalyst loading of 0.2–0.4 mg_{Pt} cm^{-2} for the cathode and 0.08 mg_{Pt} cm^{-2} for the anode, while the ionomer thickness was 4 μm. In electrochemical-performance testing, the fully IJP-

based catalyst coated membrane outscored traditionally made assemblies, even achieving a 15% higher power density(Figure 9.(b)). In summary, the development of these three approaches for multilayer manufacturing, incorporating inkjet printing, yielded uniform and high-performance CCMs compared to traditional manufacturing methods[114].

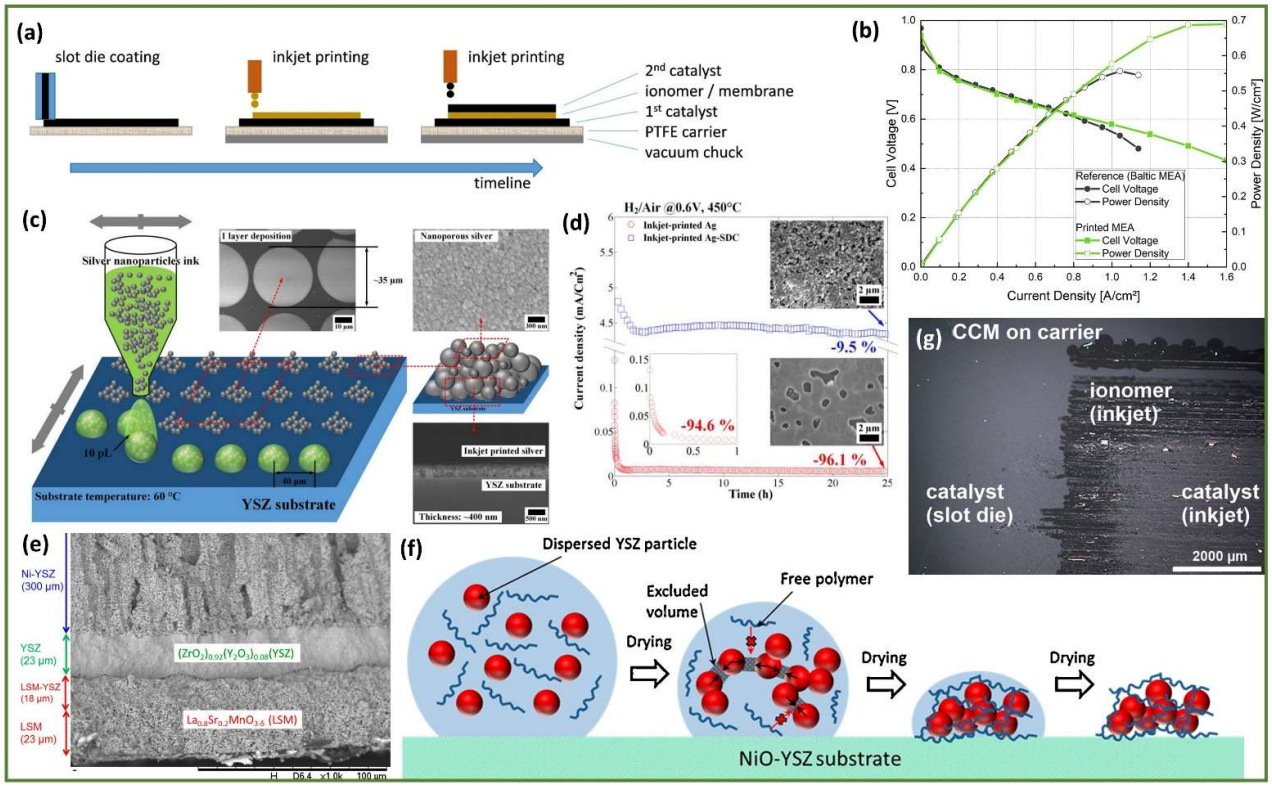

Figure 9: IJP-based fuel cells and their performances. **(a)** Combination of slot-die coating and IJP to fabricate Catalyst Coated Membranes (CCM) **(b)** Electrochemical performance comparison of an IJP-based CCM against baltic MEA **(g)** All printed layers of a CCM in sequence. Reprinted with permission from Willert et al. [114] Copyright © 2022 Elsevier B.V. **(c)** The surface morphology and cross-sectional FESEM pictures of a single printed droplet in the IJP process on a YSZ substrate **(d)** Current outputs of fuel cell with IJP-based cathodes. Reprinted with permission from Lee et al. [113] Copyright © 2017, IEEE **(e)** SEM image of Ni-YSZ/YSZ/YSZ-LSM/LSM cell cross-section post-operation **(f)** Induction of depletion potential by free polymer enhancing the drying process. Reprinted from Farandos et al. [110] under Creative Commons CC-BY license, Copyright © 2016 Elsevier B.V.

3.3.2. Fuel cells based on other printing techniques

Though IJP is the most common technique adopted for AM of fuel cells, other AM techniques such as FDM, SLA, SLS/SLM have also been explored for this purpose. In a recent study published in 2023, high resolution ceramic hierarchical lattice structures for SOFCs were developed using the micro-SLA technology, with partly stabilized ceramic (a combination of yttria-stabilized-zirconia (8YSZ) and scandia-stabilized-zirconia (6ScSZ)) as the feedstock material. Micro-CT examination indicated that the void fraction in every sample section remained below 0.15, and the surface porosity for the respective materials ranged from approximately 6% to 10%. In addition, this study provided the first observation of the ionic conductivity in the temperature range of 500-950°C for these samples. Preliminary tests indicate that the 6ScSZ ceramics exhibited a lower activation temperature for ionic conductivity and demonstrated lower impedance compared to 8YSZ at identical temperatures. To summarize, the current method proved AM as a feasible process for generating intermediate temperature SOFCs' next-generation ceramic electrolytes[115].

Lyons and Gould conducted a study on the utilization of Direct Metal Laser Sintering (DMLS) for printing titanium alloy (Ti-6Al-4V) Bipolar Plates (BPPs) at the Naval Research Laboratory (NRL). The NRL designed a BPP, featuring a serpentine flow-field and an active area of 22 cm^2. A thin coating of titanium dioxide (TiO2) was coated with gold (Au) nanoparticles before being sprayed over the BPP with a thermal spray technique to increase corrosion resistance. The rough surface of the DMLS-printed plates, which contributed to high interfacial resistance, was one important finding throughout the study. To address this issue, the plates underwent a polishing process, leading to a significant decrease in interfacial resistance[116,117]. Other techniques such as FDM or SLS have not been extensively used for fabrication of fuel cells or its components, and hence their discussion is out of the scope of this review.

Research on AM of fuel cells is still at its nascent stage and requires more effort to explore other techniques that can potentially reduce the production cost of fuel cells, which is the major concern at present.

4. Designs, Properties and Performance

As noted above, AM allows the fabrication of complex hierarchical architectures that are usually impossible to replicate via conventional manufacturing techniques. Each energy application has specific design criteria that determine its success and areas for improvement, which are influenced by the properties of the materials involved. By considering the outlined properties, it becomes possible to identify the most suitable material for a particular application. Once the materials are determined, the manufacturing process can be selected to produce the optimal material with the desired properties, aligning with the requirements of the application design. The most-common types of AM-based battery and supercapacitor electrode architectures can be observed in Figure 10.(a).This section would mainly highlight the different types of architectures possible via various AM techniques for each EESDs and discuss their effect on properties and performance of the EESDs.

4.1. Batteries

The main design configurations of 3D-printed batteries that have been explored till date are in-plane type, sandwich-type, concentric tube type and fiber-type configurations. Every configuration affects the properties and performance of the fabricated EESDs, which in turn decides their application areas. Sandwich-type and in-plane type designs (Figure 10.(c)) are the most explored battery configuration, with the sandwich-type one being cost effective and having potential for industrial scalability. It has also been commonly observed that EESDs fabricated using DIW and IJP show mostly in-plane type designs, and those fabricated by FDM/SLA based printing mostly have sandwich-type designs[118]. The microlattice electrode pattern is commonly utilized in the fabrication of 3D printed sandwich-type devices due to its advantageous properties such as high areal energy density and high-rate performance. This electrode structure consists of stacked layered filaments that form well-defined periodic macropores[119]. An additively-manufactured artificial rGO/CNT micro-lattice aerogel was fabricated for metallic sodium anode for applications in sodium metal batteries(Figure 10.(d)). The microlattice structure provided ample active nucleation sites, leading to uniform deposition of sodium to eliminate any dendrite formation. The resultant anode reported a capacity of 67.6 mAh g^{-1} at 100 mA g^{-1} after 100 cycles (Figure 10.(e))[120].

The in-plane type design is a conventional configuration used in 3D-printed batteries, where small electrodes are arranged parallel to each other on a substrate within the same plane. This design allows for compact integration of microelectrodes, and the size and spacing of the electrodes can be precisely controlled using AM. The arrangement of microscale electrodes facilitates the movement of ions due to the unique structure of these electrodes with a high aspect ratio. On contrary, the concentric tube-type arrangement represents a unique layout observed in 3D micro-batteries. This design involves a

collection of vertically aligned electrode posts that are uniformly coated with a solid electrolyte layer, while the interstitial spaces between the posts are occupied by counter electrode materials. One of the few examples of concentric tube configuration are 3D microbatteries developed by Cohen et al., where they examined the feasibility of multiple array configurations such as pentagonal, triangular or cylindrical[73].

The fiber-type configuration represents another unique battery design, where a core electrode (anode) takes the form of a cable-like structure, surrounded by an outer electrode (cathode) in a tubular shape, similar to the design of an optical fiber. Alternatively, two wire-shaped electrodes can be twisted together to form this configuration. This type of configuration has gained popularity recently owing to the hype about flexible wearable electronics[121]. Praveen et al. recently fabricated twisted yarn-type LIBs via DIW technique and conducted a detailed analysis of the rheological behavior of the different combinations of the inks formulated and electronic properties of the manufactured fibers (Figure 10.(b)). The electrode inks used in this process contained vapor-grown carbon fibers (VGCFs) and PVDF as the primary components, creating a conductive matrix. To achieve the desired properties, the inks are further enriched with carefully selected active materials such as lithium nickel cobalt manganese oxide ($LiNi_{0.6}Co_{0.2}Mn_{0.2}O_2$, NCM-622) and graphite. Upon contact with an ethanol solution in the coagulation bath, the electrode inks undergo a transformation into fibrous gels, wherein the PVDF encapsulates micro- and nanoparticles. The resulting cathode and anode fibers are individually printed and then collected. These fibers are subsequently twisted together in an axial fashion to create the cathode and anode yarns for the battery. The initial performance of the fully assembled cell exhibited specific charge and discharge capacities of 210 and 172 mAh g^{-1}, respectively. The developed cell demonstrated a discharge capacity of 166 mAh g^{-1} at 0.1 C current density[122].

Some of the common architectures used in design of additively-manufactured batteries are traditional planar architecture, hierarchical octet-truss architecture, through-thickness aligned structure, fibric architecture and interdigitated architecture[123]. The most widely used structure among the above mentioned architectures is the traditional planar architecture. Hierarchical octet-truss structure is one type of hierarchical porous structure that exhibit exceptional mechanical and electrochemical properties, as the inherent porosity in the structure help in electron distribution and mitigate the mechanical stresses among the electrodes. As an example, the hierarchical porous lattice grid structure, characterized by a series of intersecting lines, is extensively employed in the production of 3D ordered porous electrodes. This structure offers several benefits, including a high surface area and faster diffusion for electrolyte ions. The engineered hierarchical micro-lattice arrangement encourages the penetration of electrolyte ions within the electrodes, while the higher surface-to-volume ratio improves the utilization of active materials. As a result, even at high speeds, thick electrodes can operate superbly thanks to this arrangement. Moreover, 3D printing methods like DIW and FDM make it simple to fabricate the hierarchical porous microlattice structure[124]. Traditional planar structure electrodes suffer from high tortuosity, limiting the use of active materials and causing high impedance. This leads to restricted energy storage and rapid electrode degradation. In contrast, through-thickness aligned structures reduce tortuosity, enabling efficient transport of ions and electrons. This improves power density, while increased electrode thickness enhances energy density. Thus, through-thickness aligned structures offer both high energy and power density in battery and supercapacitor applications. In a recent study published a few months ago, the authors reported a novel technique for AM of through-thickness electrodes. They have implemented a novel approach that combines orientation of nanomaterials with AM, resulting in a dry electrode processing technique called structured electrode additive manufacturing (SEAM). This method allows for the rapid fabrication of thick having out-of-plane through-thickness architecture, characterized by low tortuosity and excellent mechanical strength. SEAM employs a regulated flow of molten feedstock to align materials with anisotropic properties at different scales,

facilitating efficient transport and insertion of Li-ion. The structured electrodes, with a thickness of 1 mm, exhibit more than double the specific capacity at 1 C compared to electrodes produced using slurry-casting methods. Additionally, these electrodes showcase exceptional mechanical characteristics, surpassing the performance of previously documented 3D-printed electrodes[125].

Another common electrode structure, the interdigitated structure electrode consists of closely interconnected "fingers" of each electrode, creating an interleaved pattern. This configuration notably enhances the electrode-electrolyte contact area and reduces the distance for ion transfer, leading to decreased conductive resistance. Unlike planar structure electrodes which can be fabricated using both conventional and additive manufacturing techniques, interdigitated electrodes require 3D printing methods for fabrication. Among these methods, DIW is commonly used due to its simplicity and the ability to adjust the active materials for ink printing. Numerous examples of interdigitated electrode architecture have already been mentioned in the previous sections.

The battery configuration and architecture are important parameters that affect its performance, especially when additively-manufactured batteries are considered. AM offers freedom to researchers to tune their design without pondering about the production time and cost. The use of AM to create electrode architectures also offers several advantages for increasing the capacity, energy density, and power density of batteries. These advantages result from the 3D electrodes' high areal-loading density and high aspect ratio. Additionally, one can choose to optimize the battery's areal energy density or power density by carefully choosing the thickness and porosity of the 3D-printed electrodes. The major properties that affect the electrode performance are thickness, porosity, particle size and pore size of the particular architecture[126]. For instance, in a study by Wei et al.[127], they achieved a gradual increase in electrode thickness by adjusting the number of printed layers. Because of this, the printed LIBs with ultrathick electrodes showed exceptional areal energy densities of up to 20 mWh/cm^2, far exceeding those of thin electrodes (which are typically around 1 mWh/cm^2). Additionally, the 3D-printed electrodes have a three-dimensional, high aspect-ratio architecture in contrast to conventional 2D planar electrodes. Due to shorter Li-ion and electron transport channels made possible by this characteristic, the power density of the batteries has increased. The bespoke work on through-thickness electrode architecture can be considered as an example for this case. n their method, they introduced a considerable amount of graphite flakes into a melted polymer matrix and extruded the blend. The intentional graphite flakes alignment in the printing direction was accomplished using a high-pressure-induced shear flow, which enabled the formation of interconnected channels and the orientation of graphite flakes uniformly across the cross-section. This strategic alignment process aimed to minimize the winding paths for lithium-ion movement by reducing the tortuosity within the electrode structure. As a result, the ion mobility within the electrode was significantly improved, enabling enhanced access to favorable intercalation sites within the graphite flakes. These combined effects contributed to notable advancements in both the power and energy performance of thick electrodes. The electrode alignment was achieved across multiple length scales in the through-thickness direction, enabling the establishment of the most direct pathways for efficient ion transport, ultimately resulting in enhanced overall efficiency. Consequently, the electrode exhibited a significant improvement in both specific and areal capacities at high current rates, demonstrating the effectiveness of AM in manufacturing batteries with complex architectures[125].

The pore size's influence on the properties of electrodes and lithium-ion battery (LIB) performance is often overlooked compared to factors like electrode thickness and porosity. However, pore size can have significant effects on additively-manufactured battery performance. Smaller pore sizes in electrodes, at a given porosity, lead to low tortuosity and improved ionic transport through electrolyte-filled pores. The impact of pore size on wettability is also expected to be significant. Unfortunately, pore size control and measurement pose challenges due to the interstitial nature of conventional electrode pores.

Particle size also plays a crucial role in electrode properties. The diffusion length of lithium ions in the solid state is directly influenced by the active materials' particle size. Longer diffusion lengths are known to restrict LIB performance due to larger particle sizes, especially in thin electrodes. On the other hand, using nanoscale particles can help you achieve fast charging and discharging rates. However, reducing particle size increases the electrode surface area, improving mass transfer rates but also leading to increased side reactions and higher lithium ion consumption. Additionally, small particles have low tap density, which diminishes volumetric energy density[126]. In summary, while electrode thickness, porosity, and particle size receive considerable attention, pore size's impact on electrode properties and LIB performance is often underestimated. Understanding and controlling pore size can enhance ionic transport and wettability, while optimizing particle size balances diffusion length, mass transfer rates, side reactions, and volumetric energy density.

Though designs and architectures of AM batteries were chosen with an aim to examine the feasibility of various techniques, the recent publications focus more on a problem-oriented and practical approach while deciding the battery architecture. Since DIW, IJP, FDM, SLA are some of the most common techniques for AM of EESDs, a plethora of electrode designs have been explored and fabricated in these domains, which aim to solve specific scientific problems associated with next-generation batteries. One such example is solid-state batteries utilizing solid-state electrolytes, which has already been discussed in detail in the previous section. Another optimized design strategy is developing designs that help mitigate the issues related to uncontrollable dendritic growth associated with oxidation of Li metal anode. Recently, a team led by Lee developed a UV polymerization-assisted printing technique to create an innovative solid electrolyte interphase (pSEI) mimic on Li surfaces. The formed pSEI consisted of both organic and inorganic constituents, where the organic component acted as a moisture-resistant framework, and the inorganic component facilitated efficient Li ion transport. The Li metal anode exhibited exceptional resistance to oxidation and demonstrated reliable performance in full cell tests even when exposed to humid environments. The in-situ UV polymerization process, occurring rapidly during printing, effectively prevented the oxidation of the Li anode itself, proving to be more effective than traditional methods in creating an extra SEI layer for the anodes[128].

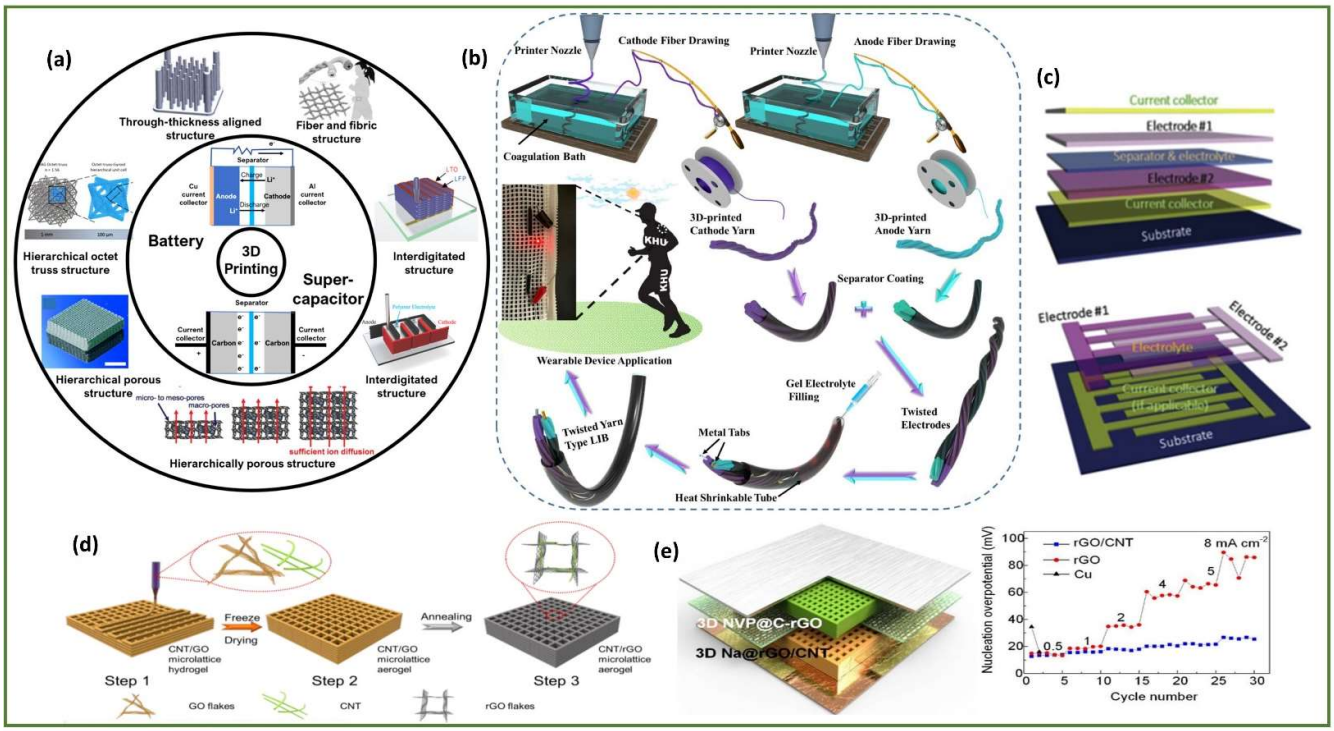

Figure 10: Various designs and configurations of AM-based batteries and supercapacitors. **(a)** Overview of AM-based electrode architectures. Reprinted from [129] under Creative Commons CC-BY license, Copyright © 2021 John Wiley & Sons **(b)** Schematic of fabrication of twisted-yarn-type LIBs. Reprinted with permission from Praveen et al. [122] Copyright © 2021, Elsevier B.V. **(c)** Sandwiched and in-plane type configurations. Reprinted from [118] under Creative Commons CC-BY license, Copyright © 2020 Elsevier B.V. **(d)** Fabrication of 3D printed rGO/CNT microlattice **(e)** microlattice aerogel used as host of sodium anode and its electrochemical performance. Reproduced with permission from Yan et al. [120] Copyright © 2020 Royal Society of Chemistry.

4.2.Supercapacitors

The electrode configurations, designs and architectures for supercapacitors are similar to that of batteries as discussed in the preceding section, only with subtle differences. The details of architectures and designs will not be reiterated in this section and emphasis will be given mainly on the electrode design's effect on the properties and performance of the fabricated supercapacitors. In order to increase the power and energy density of supercapacitors, it is crucial to design electrodes for MSCs that facilitate efficient ionic and electronic current flow.The conventional thick film electrode suffers from limited pathways for both ionic and electronic current, resulting in surface-limited electrode/electrolyte interactions. Much like the surface-type electrode, the bulk-type electrode experiences concentrated charge accumulation or redox reactions solely on its top surface, which hinders ion diffusion towards current collectors. This results in decreased electrochemical reaction efficiency. Additionally, ion diffusion into the electrode material is constrained by insufficient wetting of the electrolyte inside the electrode. The needed high energy and power density cannot be attained by these ineffective electrodes with small surface surfaces[130]. To address these challenges, researchers have explored the use of 3D nanostructured materials as active materials for MSCs electrodes to enhance its efficiency.

Another significant advantage of 3D printed electrodes for MSCs is their ability to create interconnected monolithic structures with a porous configuration, resulting in a high specific surface area. Traditional slurry-based electrodes exhibit high interfacial electrical resistance between nanoparticles, leading to low capacitance. To address this issue, scaffolding techniques are employed which involve coating a conductive 3D framework

with 1D nanostructured materials, enabling higher surface area and promoting robust redox reactions, thereby increasing the specific capacitance in MSCs. Carbon-based materials used in EDLCs (Electric Double-Layer Capacitors) demonstrate enhanced specific capacitance with increased specific surface area [131].Hierarchical electrodes can be seen as a specialized form of scaffolding, combining the advantages of interdigitated microstructures and nanoscale surface treatment, further optimizing electrode density. The monolithic 3D electrode provides efficient pathways for electrons, minimizing interfacial resistance and facilitating rapid charge carrier transport from bottom to top. This significantly improves the performance efficiency of MSCs, as conventional high aspect ratio 3D electrodes suffer from efficiency losses due to the fact that electron transportation is restricted to only one direction[130].

Some of the most common electrode structures that have been explored for supercapacitors are thin-film structure and other lattice structures like octet-truss, auxetic and cubic lattice architectures[132]. Thin films structures are most commonly found in supercapacitors due to their ease of fabrication, high surface area, and flexibility. Usually, they are fabricated using IJP or AJP methods and assembled into sandwich-type SCs. However, as the electrodes increase in thickness, the random arrangement of active components results in a complicated pore structure, which restricts ion diffusion. Therefore, it becomes necessary to produce alternative intricate lattice structures. This structure is widely employed in 3D printed SCs due to its simple unit cell design. For example, Yao et al.[133] printed macroporous graphene aerogels with a cubic lattice structure, serving as scaffolds to support active materials like MnO_2 with a high mass loading of 182.2 mg cm^{-2}. The specifically engineered porous architecture facilitated effective ion diffusion and enabled a substantial mass loading while maintaining excellent capacitive performance. In present times, there has been an increasing interest in utilizing auxetic lattice structures, which possess a unique NPR, renowned for their remarkable stretchability and flexibility. Unlike conventional materials that typically expand vertically and contract laterally when subjected to vertical tension, auxetic structures exhibit the opposite behavior. In a collaborative approach combining AM and pattern design, Chang et al. [98] printed electrodes with various NPR structures and investigated their behavior under various deformation conditions. They used DIW to fabricate four types of NPR structures, including re-entrant, S-hinged, chiral, and wavy mesh structures. Further tensile testing and FEA studies revealed that the wave mesh structure exhibited the highest maximum stress, while the S-hinged geometry had the lowest maximum stress.

Other lattice structures, such as the octet-truss lattice structure and the gyroid lattice structure, are also utilized in the design of AM-based electrodes due to their strength and toughness. In a very recent work published in February 2023, Congjian Lin and his co-authors developed 3D-printed stretchable MSCs having an octet-truss lattice structure via the DLP technique. The implementation of octet-truss electrode (OTE) MSCs results in improved electrochemical performance compared to other designs, as evidenced by larger closed areas in cyclic voltammetry profiles and longer discharge times. This enhancement in capacitance is attributed to the increased open space and electrode-electrolyte interface formation, which exhibits a positive correlation with surface area. The octet-truss structure, characterized by numerous struts, significantly increases the number of edges, resulting in a larger electrical field line of force compared to continuous interdigitated electrode designs. This edge-intensive configuration allows for greater ion absorption at the electrode-electrolyte interface. The mechanical stability of the MSCs is noteworthy, as they exhibit resilience under cyclic loading, enduring repeated stretching up to 50% strain for 100 cycles. The designed MSCs exhibit impressive capacitance of approximately 74.76 mF cm^{-3} at 1 mA cm^{-3} current density, even when subjected to significant mechanical deformation. Moreover, they maintain a capacitance of 19.53 mF cm−3 at a low temperature of -30 °C at a lower current density. FEA shows that the optimized 3D OTE structure provides eight times greater contact area per unit volume at the electrode-electrolyte interface compared to the conventional interdigitated electrode design[134].

The electrode configurations for AM-based supercapacitors are same as that for batteries like symmetric and asymmetric sandwich-type, fiber-shaped and interdigitated configurations. Manoj et al. successfully developed fully 3D-printed, an asymmetric sandwich-type transparent flexible SSCs utilizing a transparent dialysis membrane (DM) separator. The FT-ASSCs consisted of 3D line-patterned carbon black (CB)/Ag/CB electrodes. The construction of this layered architecture involved printing the top and bottom electrodes on both sides of the DM separator, followed by surface activation using dimethylformamide (DMF). By carefully adjusting the 3D electrodes' line pitch, the resulting ASSCs demonstrated outstanding optical transmittance of over 80%, coupled with remarkably higher areal capacitance than conventional non-transparent ASSCs[135]. Our literature survey shows that extensive research has been conducted on asymmetric sandwich-type structured SCs than its symmetric counterparts. In a recent work, symmetric sandwiched-structure supercapacitor was assembled with PVA/KOH solid state electrolyte via the DIW-based 3D printing technique. A new-type of active material for DIW ink preparation, a mixture of KCu_7S_4 nano-rods and rGO sheets was explored in this work[136].

Since the performance and properties of different electrode configurations are identical to that of batteries, the details would not be discussed to avoid redundancy.

4.3. Fuel Cells

The types of fuel cells, their conventional and additive manufacturing techniques have already been discussed in detail in Section 3. Unlike batteries and supercapacitors, 3D-printing of fuel cells is a recent venture yet to be explored and their designs differ from that of batteries and supercapacitors in many respects.

While significant efforts have been dedicated to the new material developments, there have been limited investigations into exploiting the potential performance enhancement of fuel cells through geometric modifications, largely due to the challenges associated with conventional manufacturing of intricate ceramic shapes. The fact that additive manufacturing allows the formation of complex architectures is also applicable to the case of SOFCs and PEM fuel cells as corrugated, ripple and tubular designs can be created. It is also important to highlight that SLA has proven to be a valuable tool in the design and fabrication of various types of fuel cells. This technique offers advantages in several aspects of fuel cell (both SOFCs and PEMFCs) manufacturing. Firstly, it enables the production of ceramic casings for microbial fuel cells and bipolar metal plates for PEMFCs. By incorporating fillers into the photocurable ceramics, desired mechanical properties can be achieved. Secondly, SLA facilitates the fabrication of porous electrodes by utilizing pore formers such as carbon. Additionally, it allows for post-thermal treatment to remove organic phases, resulting in the formation of pores. This technique is particularly beneficial for achieving the desired pore structure in the electrodes. Thirdly, SLA can be utilized in the creation of microchannels for laminar flow-based fuel cells. The selective engineering of ceramic surfaces through SLA enables the attainment of desired surface quality and precise control over the size of flow channels[137]. A recent study conducted in 2020 introduced a novel approach to fabricate 250 μm-thick 8YSZ electrolytes using SLA having corrugated architecture. The inclusion of corrugations inherently increased the active area by approximately 60% compared to a planar counterpart produced through the same printing technique. The positive impact of the increased area resulting from the corrugated structure was observed not only in the electrolyte but also in the electrodes, suggesting that the dominant phenomena are directly influenced by the area. Furthermore, durability tests conducted over a 600-hour period, even under high current density conditions, demonstrated remarkably low degradation in the enhanced cells. These findings can be considered a significant progress towards the development of a completely new generation of efficient SOFCs, stemming from the transition from a planar to a three-dimensional nature[138]. 3D-printed ripple-shaped electrolytes have also been investigated for enhancing the efficiency of SOFCs. The researchers utilized DLP 3D printing to create

samples of 8YSZ with varying angles for printing and subsequently analyzed their total conductivities. Furthermore, they printed ripple-shaped electrolytes with different thicknesses and assembled a prototype primary cell using NiO-8YSZ-8YSZ-LSM (Nickel Oxide-8YSZ/Lanthanum Strontium Manganite) materials. Comparing this cell with a reference flat cell of the same electrolyte thickness (~200 μm), an improvement of approximately 32% was observed. This improvement was attributed to the unique structure of the electrolyte, which featured a special patterned design. The increase in performance was primarily attributed to a 36% augmentation in the electrode-electrolyte interface resulting from the distinctive electrolyte patterned structure[139].

PEMFCs have garnered significant attention in the field of AM. This is primarily due to the complex nature of PEMFC components, which require multiple assembly steps to form a complete fuel cell. Every component of a PEMFC has its own AM technique that is best-suited for its fabrication. The performance of PEMFCs heavily relies on the fabrication techniques and structural properties of their components, particularly the carbon electrodes that are typically impregnated with platinum (Pt) catalysts. Consequently, extensive research has focused on developing efficient AM techniques for producing PEMFC electrodes, bipolar plates (BPPs), and gas diffusion layers (GDLs) with unique and specialized structures. Powder-based AM techniques have demonstrated the capability to fabricate BPPs with intricate structures, aiming to enhance the performance of PEMFCs. Similarly, AM techniques have been employed to improve the functionality of GDLs through the design of complex structures. By utilizing AM, metal alloys have been successfully printed to produce GDLs with intricate structures and superior performance in PEMFCs. Furthermore, the implementation of IJP has shown that CCM configuration offers benefits such as improved contact between catalysts and electrolyte layers, leading to enhanced ionic conductivity. Thus, IJP proved to be a time-saving approach for fabricating membrane electrode assemblies (MEAs) in PEMFCs[137]. Tubular shaped PEMFCs are one of the most common architecture types in such fuel cells. Tubular PEMFCs have demonstrated superior power densities in terms of both weight and volume compared to conventional prototypes. This geometry also holds the potential for reducing manufacturing costs by eliminating the need for end plates and/or bipolar plates. In terms of fuel cell stack design, utilizing individual tubular cells opens up possibilities for unexplored configurations with smaller sealing areas, allowing for improved access to replace defective single cells. Novel 316L stainless steel gas diffusion layers (GDLs) with different porosities were investigated for use in tubular high-temperature PEMFCs operating under concentrated phosphoric acid (H3PO4) conditions. The fuel cell employing these GDLs exhibited enhanced stability throughout a short-term testing period of 45 hours[140].

In summary, the AM techniques employed in PEMFCs, particularly in the fabrication of electrodes, BPPs, and GDLs, have received considerable attention. These techniques enable the production of components with complex structures, ultimately enhancing the performance and functionality of PEMFCs. Additionally, the utilization of IJP in the CCM configuration eliminates the need for certain post-treatment processes, streamlining the fabrication of MEAs.

5. Applications of AM-based EESDs

EESDs were primarily developed for energy storage applications and for electric vehicles. However, with the advent of wearable, flexible electronics, and Internet of Things (IoT)- based devices in the last few decades, it has become important to develop batteries and supercapacitors with flexible designs and complex architectures, an attribute that is only possible through additive manufacturing.

The field of wearable electronics is experiencing rapid growth driven by the increasing demand for personalized healthcare systems, a result of the demerits presented by an aging population. Customized designs for wearable devices are crucial due to the significant variations among individuals in the society. While conventional manufacturing approaches, such as photolithography-based semiconductor production, can produce high-

performance electronic devices, they lack the flexibility for optimized designs, which limits comfort and broader applications. Additive manufacturing methods offer the capability to create customized designs for each module of wearable devices. Wearable batteries, with their high energy storage capacity, are emerging as important energy sources. AM methods prove efficient in fabricating electrodes with customized designs for batteries, and patterning interdigital structures in supercapacitors. For instance, fused filament fabrication has been utilized to create 3D printed wearable batteries with controlled $LiClO_4$ doping ratios, resulting in enhanced interpenetrating transmission paths and channels for electrons and ions within the 3D skeleton[36]. Not only wearable batteries, but also wearable supercapacitors and fuel cells with customized and optimized designs are possible. Supercapacitors are highly desirable for applications requiring rapid charging and discharging, making them suitable for short-duration and high-power density scenarios. Their electrochemical energy storage mechanism, which does not involve intercalation, enables these capabilities. Researchers have extensively explored AM methods to create interdigital patterns for supercapacitors, taking advantage of their versatility in shaping materials. For instance, ultrathin micro-supercapacitors produced through precise laser processing achieved a remarkable 5.7 mWh/cm^3 volumetric energy density. These micro-supercapacitors have demonstrated potential for powering wearable LEDs, showcasing the capabilities of additive manufacturing techniques in advancing energy storage technology[141].

The continuous progress in smart and multifunctional materials, coupled with the growth of the Internet of Things (IoT), necessitates the development of innovative battery concepts that can seamlessly integrate into various substrates and devices. These new batteries should offer enhanced energy storage capabilities, including higher power and energy density. Printing technologies offer a promising avenue for achieving such batteries. These characteristics make printed batteries suitable for a wide range of applications, including smart cards, radio-frequency identification (RFID), portable medical diagnostic systems, and sensors. The rapid advancement of IoT has created a demand for flexible, highly customizable, lightweight battery systems that can seamlessly integrate with small electronic devices, wearables, and diverse structures[142]. The development of energy-efficient integrated circuits and wireless communication technologies has resulted in the availability of cost-effective and compact miniature devices suitable for remote sensing applications. This advancement has opened up possibilities for the creation of sensor networks consisting of multiple intelligent sensors, which enable the efficient gathering, processing, analysis, and distribution of valuable data in diverse environments. Porous ionogel flexible sensor (PIFS) having high resilience and low Young's modulus similar to human skin was fabricated via the DLP processing route for the purpose monitoring human emotions and for wearable wireless sensor applications[143].

The utilization of AM in the packaging of LIBs at the package level offers unique advantages that are challenging to replicate using other technologies. 3D printing enables the fabrication and packaging of customized LIBs with diverse patterns, making it a versatile approach. The battery package, achieved through AM processes, involves the individual printing of all components as well as the continuous printing of the entire assembly. While achieving fully printed and packaged LIBs solely through 3D printing remains a difficult endeavor, significant research has been conducted on partially printed and packaged LIBs. This approach involves leveraging 3D printing for specific aspects of LIB fabrication and packaging[144]. The studies conducted in this area highlight the potential of AM to enhance LIB manufacturing processes and enable the production of customized batteries with tailored designs and functionalities. Overall, 3D printing demonstrates great promise in advancing LIB packaging capabilities, offering opportunities for increased customization and improved manufacturing efficiency.

Solid-state batteries offer several advantages compared to LIBs for EV applications. One significant advantage is their enhanced durability, as they exhibit slower degradation rates over time. Additionally, they boast shorter charging times and pose lower safety

risks. Furthermore, solid-state batteries exhibit superior energy density, enabling them to store more energy or reduce the size of batteries. This characteristic holds great potential for electric vehicles, as battery weight and size directly impact their range. The substantial weight of traditional batteries negatively affects the vehicle's performance, making solid-state batteries a promising solution to address this limitation. Companies like Sakuu, ElectronInks and Tesla are already working towards commercialization of AM-based batteries for electric vehicles. Sakuu is employing a binder-jetting process developed by MIT named the Kavian 3D-Printing process. The company further uses a self-developed support material called PoraLyte, which can be deposited for the creation of hollow channels or voids as it burns away during sintering of the fabricated samples[145]. The hype around sustainability and electric vehicles especially in developed nations have increased the need for using AM for sustainable industrial scalability of various energy storage devices. With continuous advancement in various fields like medicine and AI, new application areas for AM-based EESDs may open up in the near future.

6. Future Scope and Prospects

Extensive research is currently underway to explore the possibilities of AM in battery manufacturing, which includes the printing of various components in battery such as interdigitated electrodes and solid electrolyte structures, as well as the potential for printing entire batteries. To fully leverage AM in the expanding field of energy storage, it is crucial to expand the range of printable materials, particularly for solid electrolytes, and establish suitable processing techniques to handle harsh environments. The development of atmosphere-controlled 3D printers and techniques tailored to industrial settings is essential not only for battery production but also for other applications. Moreover, the successful integration of multiple materials or functionally gradient materials in a multi-layered battery device necessitates a deep knowledge about the mechanical and chemical compatibility at the interface. Further investigations are needed to explore stable interfaces with strong adhesion, even without the application of external pressure. In this context, AM can serve as a valuable process for designing interfaces that minimize chemo-mechanical mismatches caused by volumetric changes during the lithium intercalation process in LIBs. It will also be crucial to conduct specific studies focusing on reducing mechanical stresses through enhanced geometric or compositional complexity.

The use of AM methods for battery fabrication holds great potential for significant advancements in the near future. Recent progress has been made in printing various battery elements, such as electrodes used with liquid electrolytes or solid electrolyte patterns assembled using traditional electrode casting methods. The progress of interdigitated electrode/electrolyte architectures is anticipated to play a pivotal role in advancing battery technology. These structures offer effective pathways for ionic diffusion within the solid electrolyte, as well as electronic and ionic transport within the electrodes. They bring about advantages like enhanced charge/discharge rates and improved battery packing efficiency. This development would require advanced 3D printing techniques and fully exploit the unique opportunities offered by this manufacturing approach[146].

In addition to the bespoke AM techniques, friction stir additive manufacturing (FSAM) has gained popularity in recent times. This method relies on the heat generated through friction between a non-consumable rotating tool and a feedstock material. This heat softens and plasticizes the material within a process chamber at elevated temperatures. Afterward, the material is deposited layer by layer, driven by a combination of compressive and shear forces. The method can build materials with high build rates and less porosity. Though no paper exists that employ this method for fabricated any EESD components at present, further investigation and experimentation in this domain is expected to lead to desirable outcomes in the near future[147].

The concept of solid electrolyte has not only proved useful for batteries, but also for fuel cells and supercapacitors, due to its added advantages over liquid electrolytes which are prone to leakage. The significance, advantages and recent studies on solid-state

electrolytes in various EESDs have been discussed in detail in Section 3.2.6. Another primary challenge in the field of energy storage lies in achieving high capacity in both area and volume at the device level while maintaining the efficiency of the manufacturing processes. To address this challenge, it is crucial to improve the speed and throughput of fabrication methods, or provide compelling evidence showcasing the advantages of novel geometric forms in terms of production time and cost[146]. Additionally, managing wetting features is essential to optimize the performance and durability of the interfaces between different materials as mentioned earlier. Considering the well-established and cost-effective nature of commercial supercapacitors, the initial applications for 3D-printed supercapacitors in the near term will likely be in niche markets that highly value geometric flexibility, such as integrated printed micro-supercapacitors, medical technology, and defense applications.

4D Printing: A recent advancement in AM known as 4D printing has emerged, where an additional dimension of time to the traditional 3D printing process is introduced. This innovation enables the creation of objects that can dynamically change their shape or behavior in response to external stimuli. By incorporating smart materials, 4D printing expands the possibilities for designing devices in various fields, including sensors, soft robotics, and shape memory materials. Though 4D printing has found applications in mainly wearable electronics and biomedical devices, few works about 4D printing of batteries and supercapacitors have been reported in the recent years. Zhou et al. have introduced a convenient method for fabricating stretchable electrodes with arbitrary shapes through 4D printing based on Aerosol Jet Printing (AJP) method, utilizing a conductive composite consisting of rGO, CNT and PEDOT:PSS. The researchers fabricated the electrodes on an extremely stretchable substrate. Their investigation centered around a recently developed composition of RGO-CNT-PEDOT:PSS solution, which acted as a printable precursor for flexible and stretchable supercapacitor electrodes. These electrodes demonstrated cyclic deformability during and after the printing process, leading to the development of a flexible electrode capable of 4D shape-morphing. The researchers optimized a methanol solution mixture of RGO-CNT-PEDOT:PSS as the ink for fabricating stretchable RGO-CNT-PEDOT:PSS-based SCs, eliminating the need for additional reduction processes. By incorporating a polymer hydrogel electrolyte, they successfully produced high-performance SSCs. These SCs demonstrated an impressive specific capacitance of 21.7 F g^{-1} at 0.5 A g^{-1} and a remarkable capacitance retention of approximately 85.8% when subjected to large biaxial strains. Notably, the 4D-printed SCs maintained their functionality and electrochemical performance even under significant cyclic mechanical deformations[148]. 4D printing can advance the field of flexible electronics, enabling the creation of complex and customizable structures that can adapt and perform reliably under various conditions. Thus, 4D printing offers a promising avenue for the fabrication of stretchable SCs with enhanced properties and opens up possibilities for future applications in wearable devices, smart textiles, and other areas where deformable energy storage systems are needed.

Biomimetic design optimization: As AM provides freedom to fabricate EESDs with complex architectures, bio-inspired designs and configurations are now being explored for optimizing the LIB performance, sodium-ion batteries, lithium-sulfur batteries. For instance, Gao et al. employed an electrodeposition method to fabricate an ordered porous metallic foam on a metal substrate, inspired from the hierarchical porous structure of a bamboo fiber. They introduced a novel approach using freeze-casting and a metal substrate with temperature gradient to produce a bamboo fiber-like porous structure in graphene aerogel (GA). This method utilized special templates, such as matter-gas and ice, which played an active role in preventing restacking and guiding the growth of highly ordered rGO fibers, resembling the structure of bamboo fibers. Through the electrodeposition method, a biomimetic and radially symmetric GA was successfully fabricated with a high level of orientation using hydrogen bubbles and ice as templates. Mechanical tests conducted at different scales demonstrated the exceptional flexibility and durability of the

GA, making it highly promising for applications in flexible electronics. Notably, the developed device exhibited a remarkable areal capacity of 7.9 mF cm^{-2} at a current density of 0.5 mA cm^{-2}, and even when the current density increased by tenfold, it maintained a capacity of 6.9 mF cm^{-2}. The GA can serve not only as a sensor electrode material and supercapacitors but also as current collector support in supercapacitors and batteries. This versatility stems from the GA's distinctive properties, making it a valuable component in energy storage devices[149]. Further, a commonly used approach for creating flexible and conductive bioelectronic materials involves the incorporation of nanomaterials into elastomer composites, known as nanocomposites. These nanocomposites typically consist of nanofilms or nanoparticles embedded within soft substrates, enabling the development of pressure and strain sensing electronics that can accurately measure local and global resistivity. In a recent research conducted by Wang et al., they employed an aramid-based nanocomposite to create a structural battery with a conformal design. The inclusion of aramid ion conductors in the nanocomposite resulted in several desirable properties, including high strength, excellent conductivity, and percolating behavior. As a result, the structural battery exhibited a remarkable battery capacity that was 72 times higher than a LIB with the same volume. This advancement highlights the potential of nanocomposites in revolutionizing energy storage systems by significantly enhancing their capacity and performance[150]. Such works contribute to the advancement of biomimetic materials and opens up possibilities for developing efficient electronic devices and energy storage systems. Though there are numerous studies on biomimetic design-based batteries/supercapacitors, such biomimetic EESDs are often not fabricated using AM techniques resulting in limited number of works in this field, despite its ease of creating complex architectures. A major reason for this issue could be lack of an interdisciplinary approach as such works require collaboration between experts in materials science, bioengineering, mechanics, and electrochemistry. Furthermore, the development of biomimetic batteries, regardless of the fabrication method, requires substantial research and development efforts. While 3D printing offers the potential for complex architectures, it is just one of several fabrication methods available. Researchers may choose alternative fabrication approaches based on their specific research goals, available resources, and expertise. However, as AM continues to advance and researchers explore new avenues for biomimetic battery designs, more studies can be expected to get published on this niche subject in the near future.

AM of EESDs in micro-gravity environment: This area is gaining attention in the research community recently with the rise of initiatives for Moon and Mars colonization and long-duration missions to such planets. AM in other planets is significantly challenging owing to the variation of process parameters in a micro-gravity environment and limitation of feedstock materials suitable for AM on these planets. NASA has been manufacturing polymer and metal parts via AM on the ISS since 2014. Astronauts aboard the ISS are also researching on leveraging the AM technologies for flexible and wearable electronics and sensor devices in a micro-gravity environment under the In-Space Manufacturing (ISM) project[151]. Moreover, in order to significantly decrease the reliance of astronauts on supplies from Earth during future missions to the Moon and Mars, it will be crucial to manufacture batteries using raw materials available on the lunar or Martian surfaces, known as in situ resource utilization (ISRU). Currently, rechargeable batteries, particularly Li-ion batteries, are used in various applications on the International Space Station, including life support systems, exploration robots and portable communication systems. However, the limited availability of Li on the Moon and Mars makes manufacturing LIBs from ISRU materials impractical. Analyzing samples collected during the previous Apollo missions, it has been found that the Moon has only trace amounts of Li (10 parts per million), while Mars also has a low calculated concentration of Li (between 1.8 and 3 parts per million). Considering the greater abundance of sodium (Na) compared to Li, Na-ion battery technology can be a more feasible alternative for battery manufacturing in lunar and Martian missions. A vital element of batteries, thermoplastic polyolefin separators, has the potential to be manufactured using recycled waste packaging materials on

celestial bodies like the Moon or Mars [152]. Considering the liquid electrolyte, $NaPF_6$ salt shows promise as a favorable choice for producing lunar batteries, primarily due to its abundant constituent materials, especially in the Moon's Maria region[152,153]. Additionally, ceramic solid electrolytes like the rhombohedral β″-Al2O3 phase present interesting possibilities due to abundant alumina on Moon and Mars. β″-Al2O3 has been studied for its high ionic conductivity in both single-crystal form (1 S cm^{-1} at 300 °C) and polycrystalline phases (0.22–0.35 S cm^{-1} at 300 °C and 2.0 mS cm^{-1} at room temperature)[152,154]. It is further predicted that early missions would exploit AM technologies to manufacture EESDs for various Lunar and Martian rovers and modules for small-scale production[152]. However, there will be a gradual shift towards traditional slurry casting process if AM processes are not efficient enough to support the growing demand of EESD with increasing interplanetary missions and colonies. The bespoke applications and future directions have been summarized in Figure 11.

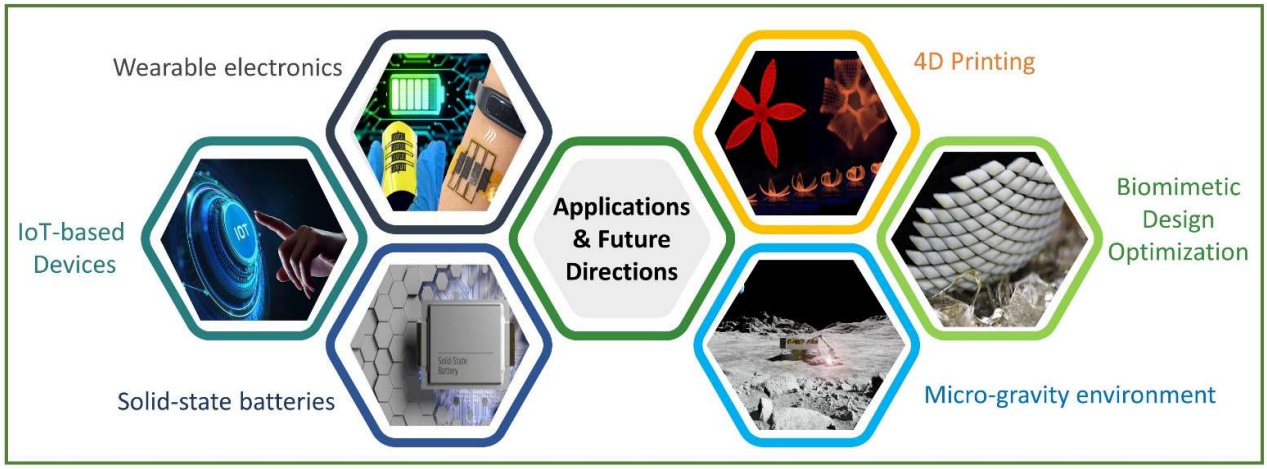

Figure 11: Applications and future directions of EESDs.

7. Summary and Conclusion

The review focused on the application of AM in the fabrication of energy storage devices. It highlighted the growing importance of energy storage in various fields, such as renewable energy integration, electric vehicles, and portable electronics. The conventional manufacturing techniques for energy storage devices face challenges in terms of customization, integration, and cost-effectiveness, which can be overcome by leveraging the capabilities of AM. The review discussed the potential of AM in fabricating EESDs mainly batteries, supercapacitors, and fuel cells. Different types of AM were explained, including the ability to create complex geometries, customize designs, and optimized performance. The various AM techniques for batteries, supercapacitors and fuel cells highlighting the printable and active materials, AM methods, post-processing techniques and electrochemical performance of the fabricated EESDs in recent studies were explored in detail. We also discussed the significance of printing solid electrolyte materials leveraging AM methods and mitigating hazards associated with conventional liquid electrolyte EESDs. Further, we discussed the numerous design configurations and architectures possible for each EESD which can lead to improved efficiency of the fabricated samples by citing recent works in this area. We also briefed about the applications of 3D-printed EESDs in a myriad of emerging fields like flexible and wearable electronics, IoT-based devices, electric vehicles, etc. by replacing traditional deposition processes. Some of the recent advances in this field were elaborated and few niche future directions which are yet to be explored such as 4D printing, biomimetic and bio-inspired design optimization using AM, and in-space manufacturing of EESDs for future space missions, were also taken into consideration and discussed briefly.

In conclusion, the comprehensive literature review highlights the progress and challenges in the field of AM for energy storage. However, some of the key challenges should be addressed in the near future to accelerate further research in this field. It is observed that 3D printing of fuel cells is still at a nascent stage and requires further research to overcome the complexities of printing multiple layers and only very few works exist that built a complete fuel cell via AM processes. The review emphasizes the need to explore alternative printing techniques like BJ and other emerging methods to expand the possibilities and overcome the limitations of current approaches. This exploration can enable the utilization of new materials and architectures, enhancing the performance and functionality of EESDs. To make the 3D printing process more sustainable, it is further encouraged to consider the recyclability of 3D-printed EESDs. Implementing recycling strategies can reduce waste and promote a circular economy for energy storage technologies. Furthermore, the review underscores the importance of adopting an interdisciplinary approach to accelerate research in this field. Collaboration between materials scientists, engineers, chemists, and other experts can foster innovative solutions and drive advancements in additive manufacturing for EESDs. Although 3D printing shows great promise for EESD fabrication, mass-scale production remains a significant challenge. Optimizing the printing technique itself, rather than solely exploring various materials and architectures, is crucial to overcome this obstacle. It is encouraging to see that some companies like Sakuu, Tesla, Electroninks are starting to explore this area, but further efforts are needed to refine the process and make it viable for large-scale production.

In summary, additive manufacturing has demonstrated its potential for revolutionizing the energy storage device fabrication. By addressing the mentioned points, including further research in fuel cells, exploring new printing techniques, considering recyclability, adopting an interdisciplinary approach, and optimizing the technique for mass production, the field can advance towards sustainable and efficient energy storage solutions.

Funding: This research received no external funding

Conflicts of Interest: The authors declare no conflict of interest.

References

[1] Battery Market Size, Share & Trends Analysis Report By Product (Lead Acid, Li-ion, Nickle Metal Hydride, Ni-Cd), By Application, By End-use, By Region, And Segment Forecasts, 2023 - 2030, (2023).

[2] M. Srivastava, S. Rathee, V. Patel, A. Kumar, P.G. Koppad, A review of various materials for additive manufacturing: Recent trends and processing issues, Journal of Materials Research and Technology. 21 (2022) 2612–2641. https://doi.org/https://doi.org/10.1016/j.jmrt.2022.10.015.

[3] D. Han, H. Lee, Recent advances in multi-material additive manufacturing: methods and applications, Curr Opin Chem Eng. 28 (2020) 158–166. https://doi.org/https://doi.org/10.1016/j.coche.2020.03.004.

[4] K. V. Wong, A. Hernandez, A Review of Additive Manufacturing, ISRN Mechanical Engineering. 2012 (2012) 1–10. https://doi.org/10.5402/2012/208760.

[5] D. Herzog, V. Seyda, E. Wycisk, C. Emmelmann, Additive manufacturing of metals, Acta Mater. 117 (2016) 371–392. https://doi.org/10.1016/j.actamat.2016.07.019.

[6] M. Jiménez, L. Romero, I.A. Domínguez, M.D.M. Espinosa, M. Domínguez, Additive Manufacturing Technologies: An Overview about 3D Printing Methods and Future Prospects, Complexity. 2019 (2019). https://doi.org/10.1155/2019/9656938.

[7] M.S. Saleh, J. Li, J. Park, R. Panat, 3D printed hierarchically-porous microlattice electrode materials for exceptionally high specific capacity and areal capacity lithium ion batteries, Addit Manuf. 23 (2018) 70–78. https://doi.org/https://doi.org/10.1016/j.addma.2018.07.006.

[8] S.A.M. Tofail, E.P. Koumoulos, A. Bandyopadhyay, S. Bose, L. O'Donoghue, C. Charitidis, Additive manufacturing: scientific and technological challenges, market uptake and opportunities, Materials Today. 21 (2018) 22–37. https://doi.org/https://doi.org/10.1016/j.mattod.2017.07.001.

[9] S. Saleh Alghamdi, S. John, N. Roy Choudhury, N.K. Dutta, Additive Manufacturing of Polymer Materials: Progress, Promise and Challenges, Polymers (Basel). 13 (2021). https://doi.org/10.3390/polym13050753.

[10] https://www.iso.org/home.html, (2010).

[11] Technology overview metal Additive Manufacturing, (n.d.).

[12] https://www.astm.org/f2792-12.html, (2012).

[13] U. Shaukat, E. Rossegger, S. Schlögl, A Review of Multi-Material 3D Printing of Functional Materials via Vat Photopolymerization, Polymers (Basel). 14 (2022).

[14] A.M.E. Arefin, N.R. Khatri, N. Kulkarni, P.F. Egan, Polymer 3D printing review: Materials, process, and design strategies for medical applications, Polymers (Basel). 13 (2021). https://doi.org/10.3390/polym13091499.

[15] O. Gülcan, K. Günaydın, A. Tamer, The state of the art of material jetting—a critical review, Polymers (Basel). 13 (2021). https://doi.org/10.3390/polym13162829.

[16] M. Ziaee, N.B. Crane, Binder jetting: A review of process, materials, and methods, Addit Manuf. (2019).

[17] H. Pinegar, Y.R. Smith, Recycling of End-of-Life Lithium Ion Batteries, Part I: Commercial Processes, Journal of Sustainable Metallurgy. 5 (2019) 402–416. https://doi.org/10.1007/s40831-019-00235-9.

[18] S.N. Bryntesen, A. Strømman, I. Tolstorebrov, P. Shearing, J. Lamb, O. Burheim, Opportunities for the State-of-the-Art Production of LIB Electrodes-A Review, Energies (Basel). 14 (2021) 1406. https://doi.org/10.3390/en14051406.

[19] H. Chen, T.N. Cong, W. Yang, C. Tan, Y. Li, Y. Ding, Progress in electrical energy storage system: A critical review, Progress in Natural Science. 19 (2009) 291–312. https://doi.org/https://doi.org/10.1016/j.pnsc.2008.07.014.

[20] U. Koehler, Chapter 2 - General Overview of Non-Lithium Battery Systems and their Safety Issues, in: J. Garche, K. Brandt (Eds.), Electrochemical Power Sources: Fundamentals, Systems, and Applications, Elsevier, 2019: pp. 21–46. https://doi.org/https://doi.org/10.1016/B978-0-444-63777-2.00002-5.

[21] G. Primavesi, Aluminium Electrolytic Capacitors, n.d. https://doi.org/10.1049/ic:19971089 (accessed May 13, 2023).

[22] A.G. Olabi, C. Onumaegbu, T. Wilberforce, M. Ramadan, M.A. Abdelkareem, A.H. Al – Alami, Critical review of energy storage systems, Energy. 214 (2021). https://doi.org/10.1016/j.energy.2020.118987.

[23] V. Mehta, J.S. Cooper, Review and analysis of PEM fuel cell design and manufacturing, J Power Sources. 114 (2003) 32–53. https://doi.org/https://doi.org/10.1016/S0378-7753(02)00542-6.

[24] X. Tian, J. Jin, S. Yuan, C.K. Chua, S.B. Tor, K. Zhou, Emerging 3D-Printed Electrochemical Energy Storage Devices: A Critical Review, Adv Energy Mater. 7 (2017). https://doi.org/10.1002/aenm.201700127.

[25] X. Gao, M. Zheng, X. Yang, R. Sun, J. Zhang, X. Sun, Emerging application of 3D-printing techniques in lithium batteries: From liquid to solid, Materials Today. 59 (2022) 161–181. https://doi.org/https://doi.org/10.1016/j.mattod.2022.07.016.

[26] Y. Pang, Y. Cao, Y. Chu, M. Liu, K. Snyder, D. MacKenzie, C. Cao, Additive Manufacturing of Batteries, Adv Funct Mater. 30 (2020). https://doi.org/10.1002/adfm.201906244.

[27] 3D-printed Battery Market, (2022).

[28] J. Huang, J. Yang, W. Li, W. Cai, Z. Jiang, Electrochemical properties of LiCoO2 thin film electrode prepared by ink-jet printing technique, Thin Solid Films. 516 (2008) 3314–3319. https://doi.org/https://doi.org/10.1016/j.tsf.2007.09.039.

[29] K. Sun, T.S. Wei, B.Y. Ahn, J.Y. Seo, S.J. Dillon, J.A. Lewis, 3D printing of interdigitated Li-ion microbattery architectures, Advanced Materials. 25 (2013) 4539–4543. https://doi.org/10.1002/adma.201301036.

[30] C. Zhao, C. Wang, R. Gorkin, S. Beirne, K. Shu, G.G. Wallace, Three dimensional (3D) printed electrodes for interdigitated supercapacitors, Electrochem Commun. 41 (2014) 20–23. https://doi.org/https://doi.org/10.1016/j.elecom.2014.01.013.

[31] K. Fu, Y. Wang, C. Yan, Y. Yao, Y. Chen, J. Dai, S. Lacey, Y. Wang, J. Wan, T. Li, Z. Wang, Y. Xu, L. Hu, Graphene Oxide-Based Electrode Inks for 3D-Printed Lithium-Ion Batteries, Advanced Materials. 28 (2016) 2587–2594. https://doi.org/10.1002/adma.201505391.

[32] R.R. Kohlmeyer, A.J. Blake, J.O. Hardin, E.A. Carmona, J. Carpena-Núñez, B. Maruyama, J. Daniel Berrigan, H. Huang, M.F. Durstock, Composite batteries: A simple yet universal approach to 3D printable lithium-ion battery electrodes, J Mater Chem A Mater. 4 (2016) 16856–16864. https://doi.org/10.1039/c6ta07610f.

[33] H. Ning, J.H. Pikul, R. Zhang, X. Li, S. Xu, J. Wang, J.A. Rogers, W.P. King, P. V. Braun, Holographic patterning of high-performance on-chip 3D lithium-ion microbatteries, Proc Natl Acad Sci U S A. 112 (2015) 6573–6578. https://doi.org/10.1073/pnas.1423889112.

[34] A. Azhari, E. Marzbanrad, D. Yilman, E. Toyserkani, M.A. Pope, Binder-jet powder-bed additive manufacturing (3D printing) of thick graphene-based electrodes, Carbon N Y. 119 (2017) 257–266. https://doi.org/https://doi.org/10.1016/j.carbon.2017.04.028.

[35] D.X. Luong, A.K. Subramanian, G.A.L. Silva, J. Yoon, S. Cofer, K. Yang, P.S. Owuor, T. Wang, Z. Wang, J. Lou, P.M. Ajayan, J.M. Tour, Laminated Object Manufacturing of 3D-Printed Laser-Induced Graphene Foams, Advanced Materials. 30 (2018). https://doi.org/10.1002/adma.201707416.

[36] C. Reyes, R. Somogyi, S. Niu, M.A. Cruz, F. Yang, M.J. Catenacci, C.P. Rhodes, B.J. Wiley, Three-Dimensional Printing of a Complete Lithium Ion Battery with Fused Filament Fabrication, ACS Appl Energy Mater. 1 (2018) 5268–5279. https://doi.org/10.1021/acsaem.8b00885.

[37] S.H. Park, M. Kaur, D. Yun, W.S. Kim, Hierarchically Designed Electron Paths in 3D Printed Energy Storage Devices, Langmuir. 34 (2018) 10897–10904. https://doi.org/10.1021/acs.langmuir.8b02404.

[38] J. Xue, L. Gao, X. Hu, K. Cao, W. Zhou, W. Wang, Y. Lu, Stereolithographic 3D Printing-Based Hierarchically Cellular Lattices for High-Performance Quasi-Solid Supercapacitor, Nanomicro Lett. 11 (2019) 46. https://doi.org/10.1007/s40820-019-0280-2.

[39] Z. Fan, C. Wei, L. Yu, Z. Xia, J. Cai, Z. Tian, G. Zou, S.X. Dou, J. Sun, 3D Printing of Porous Nitrogen-Doped Ti3C2 MXene Scaffolds for High-Performance Sodium-Ion Hybrid Capacitors, ACS Nano. 14 (2020) 867–876. https://doi.org/10.1021/acsnano.9b08030.

[40] A.D. Taylor, E.Y. Kim, V.P. Humes, J. Kizuka, L.T. Thompson, Inkjet printing of carbon supported platinum 3-D catalyst layers for use in fuel cells, J Power Sources. 171 (2007) 101–106. https://doi.org/https://doi.org/10.1016/j.jpowsour.2007.01.024.

[41] V. Esposito, C. Gadea, J. Hjelm, D. Marani, Q. Hu, K. Agersted, S. Ramousse, S.H. Jensen, Fabrication of thin yttria-stabilized-zirconia dense electrolyte layers by inkjet printing for high performing solid oxide fuel cells, J Power Sources. 273 (2015) 89–95. https://doi.org/https://doi.org/10.1016/j.jpowsour.2014.09.085.

[42] J.A. Lewis, Direct ink writing of 3D functional materials, Adv Funct Mater. 16 (2006) 2193–2204. https://doi.org/10.1002/adfm.200600434.

[43] Cheng Zhu, James E. Smay, Thixotropic rheology of concentrated alumina colloidal gels for solid freeform fabrication, J Rheol (N Y N Y). 55 (2011).

[44] P. Coussot, Yield stress fluid flows: A review of experimental data, J Nonnewton Fluid Mech. 211 (2014) 31–49. https://doi.org/https://doi.org/10.1016/j.jnnfm.2014.05.006.

[45] J.H. Kim, S. Lee, M. Wajahat, H. Jeong, W.S. Chang, H.J. Jeong, J.-R. Yang, J.T. Kim, S.K. Seol, Three-Dimensional Printing of Highly Conductive Carbon Nanotube Microarchitectures with Fluid Ink, ACS Nano. 10 (2016) 8879–8887. https://doi.org/10.1021/acsnano.6b04771.

[46] S. Tagliaferri, A. Panagiotopoulos, C. Mattevi, Direct ink writing of energy materials, Mater Adv. 2 (2021) 540–563. https://doi.org/10.1039/d0ma00753f.

[47] A. M'Barki, L. Bocquet, A. Stevenson, Linking Rheology and Printability for Dense and Strong Ceramics by Direct Ink Writing, Sci Rep. 7 (2017) 6017. https://doi.org/10.1038/s41598-017-06115-0.

[48] S.D. Lacey, D.J. Kirsch, Y. Li, J.T. Morgenstern, B.C. Zarket, Y. Yao, J. Dai, L.Q. Garcia, B. Liu, T. Gao, S. Xu, S.R. Raghavan, J.W. Connell, Y. Lin, L. Hu, Extrusion-Based 3D Printing of Hierarchically Porous Advanced Battery Electrodes, Advanced Materials. 30 (2018) 1705651. https://doi.org/https://doi.org/10.1002/adma.201705651.

[49] Y.Z. Zhang, Y. Wang, Q. Jiang, J.K. El-Demellawi, H. Kim, H.N. Alshareef, MXene Printing and Patterned Coating for Device Applications, Advanced Materials. 32 (2020). https://doi.org/10.1002/adma.201908486.

[50] C. Chen, X. Xie, B. Anasori, A. Sarycheva, T. Makaryan, M. Zhao, P. Urbankowski, L. Miao, J. Jiang, Y. Gogotsi, MoS 2 -on-MXene Heterostructures as Highly Reversible Anode Materials for Lithium-Ion Batteries , Angewandte Chemie. 130 (2018) 1864–1868. https://doi.org/10.1002/ange.201710616.

[51] H. Tang, W. Li, L. Pan, C.P. Cullen, Y. Liu, A. Pakdel, D. Long, J. Yang, N. McEvoy, G.S. Duesberg, V. Nicolosi, C. (John) Zhang, In Situ Formed Protective Barrier Enabled by Sulfur@Titanium Carbide (MXene) Ink for Achieving High-Capacity, Long Lifetime Li-S Batteries, Advanced Science. 5 (2018). https://doi.org/10.1002/advs.201800502.

[52] P. Yang, H.J. Fan, Inkjet and Extrusion Printing for Electrochemical Energy Storage: A Minireview, Adv Mater Technol. 5 (2020). https://doi.org/10.1002/admt.202000217.

[53] N. Reis, B. Derby, Ink Jet Deposition of Ceramic Suspensions: Modeling and Experiments of Droplet Formation, MRS Proceedings. 625 (2000) 117. https://doi.org/10.1557/PROC-625-117.

[54] P. Yang, H.J. Fan, Inkjet and Extrusion Printing for Electrochemical Energy Storage: A Minireview, Adv Mater Technol. 5 (2020) 2000217. https://doi.org/https://doi.org/10.1002/admt.202000217.

[55] R.D. Deegan, O. Bakajin, T.F. Dupont, G. Huber, S.R. Nagel, T.A. Witten, Capillary flow as the cause of ring stains from dried liquid drops, Nature. 389 (1997) 827–829. https://doi.org/10.1038/39827.

[56] P.J. Yunker, T. Still, M.A. Lohr, A.G. Yodh, Suppression of the coffee-ring effect by shape-dependent capillary interactions, Nature. 476 (2011) 308–311. https://doi.org/10.1038/nature10344.

[57] M. Majumder, C.S. Rendall, J.A. Eukel, J.Y.L. Wang, N. Behabtu, C.L. Pint, T.-Y. Liu, A.W. Orbaek, F. Mirri, J. Nam, A.R. Barron, R.H. Hauge, H.K. Schmidt, M. Pasquali, Overcoming the "Coffee-Stain" Effect by Compositional Marangoni-Flow-Assisted Drop-Drying, J Phys Chem B. 116 (2012) 6536–6542. https://doi.org/10.1021/jp3009628.

[58] T. Janoschka, A. Teichler, B. Häupler, T. Jähnert, M.D. Hager, U.S. Schubert, Reactive inkjet printing of cathodes for organic radical batteries, Adv Energy Mater. 3 (2013) 1025–1028. https://doi.org/10.1002/aenm.201300036.

[59] P.-E. Delannoy, B. Riou, T. Brousse, J. Le Bideau, D. Guyomard, B. Lestriez, Ink-jet printed porous composite LiFePO4 electrode from aqueous suspension for microbatteries, J Power Sources. 287 (2015) 261–268. https://doi.org/https://doi.org/10.1016/j.jpowsour.2015.04.067.

[60] S. Lawes, Q. Sun, A. Lushington, B. Xiao, Y. Liu, X. Sun, Inkjet-printed silicon as high performance anodes for Li-ion batteries, Nano Energy. 36 (2017) 313–321. https://doi.org/https://doi.org/10.1016/j.nanoen.2017.04.041.

[61] P. Chang, H. Mei, S. Zhou, K.G. Dassios, L. Cheng, 3D printed electrochemical energy storage devices, J Mater Chem A Mater. 7 (2019) 4230–4258. https://doi.org/10.1039/c8ta11860d.

[62] P.-E. Delannoy, B. Riou, B. Lestriez, D. Guyomard, T. Brousse, J. Le Bideau, Toward fast and cost-effective ink-jet printing of solid electrolyte for lithium microbatteries, J Power Sources. 274 (2015) 1085–1090. https://doi.org/https://doi.org/10.1016/j.jpowsour.2014.10.164.

[63] Y. Gu, J.F. Federici, Fabrication of a flexible current collector for lithium ion batteries by inkjet printing, Batteries. 4 (2018). https://doi.org/10.3390/batteries4030042.

[64] E. Brown, P. Yan, H. Tekik, A. Elangovan, J. Wang, D. Lin, J. Li, 3D printing of hybrid MoS2-graphene aerogels as highly porous electrode materials for sodium ion battery anodes, Mater Des. 170 (2019) 107689. https://doi.org/https://doi.org/10.1016/j.matdes.2019.107689.

[65] Dong Wen, Guobing Ying, Lu Liu, Cheng Sun, Yuexia Li, Yinlong Zhao, Xiang Wang, Flexible and High-Performance MXene/MnO2 Film Electrodes Fabricated by Inkjet Printing: Toward a New Generation Supercapacitive Application, Adv Mater Interfaces. 8 (2021).

[66] H. Sirringhaus, T. Shimoda, Inkjet Printing of Functional Materials, MRS Bull. 28 (2003) 802–806. https://doi.org/10.1557/mrs2003.228.

[67] S.C. Ligon, R. Liska, J. Stampfl, M. Gurr, R. Mülhaupt, Polymers for 3D Printing and Customized Additive Manufacturing, Chem Rev. 117 (2017) 10212–10290. https://doi.org/10.1021/acs.chemrev.7b00074.

[68] H.H. Bin Hamzah, O. Keattch, D. Covill, B.A. Patel, The effects of printing orientation on the electrochemical behaviour of 3D printed acrylonitrile butadiene styrene (ABS)/carbon black electrodes, Sci Rep. 8 (2018). https://doi.org/10.1038/s41598-018-27188-5.

[69] J. Zhang, B. Yang, F. Fu, F. You, X. Dong, M. Dai, Resistivity and Its Anisotropy Characterization of 3D-Printed Acrylonitrile Butadiene Styrene Copolymer (ABS)/Carbon Black (CB) Composites, Applied Sciences. 7 (2017). https://doi.org/10.3390/app7010020.

[70] M.N. Hafsa, M. Ibrahim, M.S. Wahab, M.S. Zahid, Evaluation of FDM pattern with ABS and PLA material, in: Applied Mechanics and Materials, 2014: pp. 55–59. https://doi.org/10.4028/www.scientific.net/AMM.465-466.55.

[71] K. Ghosh, S. Ng, C. Iffelsberger, M. Pumera, 2D MoS2/carbon/polylactic acid filament for 3D printing: Photo and electrochemical energy conversion and storage, Appl Mater Today. 26 (2022) 101301. https://doi.org/https://doi.org/10.1016/j.apmt.2021.101301.

[72] Stereolithography Apparatus, Https://3faktur.Com/En/3d-Printing-Materials-Technologies/Stereolithography-Sla-Technology-Overview/#1481032334093-9c9cb5b4-6e92. (n.d.).

[73] E. Cohen, S. Menkin, M. Lifshits, Y. Kamir, A. Gladkich, G. Kosa, D. Golodnitsky, Novel rechargeable 3D-Microbatteries on 3D-printed-polymer substrates: Feasibility study, Electrochim Acta. 265 (2018) 690–701. https://doi.org/https://doi.org/10.1016/j.electacta.2018.01.197.

[74] Chen Li, Junjie Du, Yong Gao, Fan Bu, Yong Hao Tan, Yuxuan Wang, Gangwen Fu, Cao Guan, Xi Xu, Wei Huang, Stereolithography of 3D Sustainable Metal Electrodes towards High-Performance Nickel Iron Battery, Adv Funct Mater. 32 (2022).

[75] M.D. Reale Batista, S. Chandrasekaran, B.D. Moran, M. Salazar de Troya, A. Pinongcos, Z. Wang, R. Hensleigh, A. Carleton, M. Zeng, T. Roy, D. Lin, X. Xue, V.A. Beck, D.A. Tortorelli, M. Stadermann, R. Zheng, Y. Li, M.A. Worsley, Design and additive manufacturing of optimized electrodes for energy storage applications, Carbon N Y. 205 (2023) 262–269. https://doi.org/https://doi.org/10.1016/j.carbon.2023.01.044.

[76] K.A. Acord, A.D. Dupuy, U. Scipioni Bertoli, B. Zheng, W.C. West, Q.N. Chen, A.A. Shapiro, J.M. Schoenung, Morphology, microstructure, and phase states in selective laser sintered lithium ion battery cathodes, J Mater Process Technol. 288 (2021). https://doi.org/10.1016/j.jmatprotec.2020.116827.

[77] W. Zhang, H. Liu, X. Zhang, X. Li, G. Zhang, P. Cao, 3D Printed Micro-Electrochemical Energy Storage Devices: From Design to Integration, Adv Funct Mater. 31 (2021). https://doi.org/10.1002/adfm.202104909.

[78] S. Wang, Y. Yu, R. Li, G. Feng, Z. Wu, G. Compagnini, A. Gulino, Z. Feng, A. Hu, High-performance stacked in-plane supercapacitors and supercapacitor array fabricated by femtosecond laser 3D direct writing on polyimide sheets, Electrochim Acta. 241 (2017) 153–161. https://doi.org/https://doi.org/10.1016/j.electacta.2017.04.138.

[79] F. Zhang, Z. Li, M. Xu, S. Wang, N. Li, J. Yang, A review of 3D printed porous ceramics, J Eur Ceram Soc. 42 (2022) 3351–3373. https://doi.org/https://doi.org/10.1016/j.jeurceramsoc.2022.02.039.

[80] B. Mueller, D. Kochan, Laminated object manufacturing for rapid tooling and patternmaking in foundry industry, Comput Ind. 39 (1999) 47–53. https://doi.org/https://doi.org/10.1016/S0166-3615(98)00127-4.

[81] S. Meteyer, X. Xu, N. Perry, Y.F. Zhao, Energy and material flow analysis of binder-jetting additive manufacturing processes, in: Procedia CIRP, Elsevier B.V., 2014: pp. 19–25. https://doi.org/10.1016/j.procir.2014.06.030.

[82] A. Kumar, S. Mandal, S. Barui, R. Vasireddi, U. Gbureck, M. Gelinsky, B. Basu, Low temperature additive manufacturing of three dimensional scaffolds for bone-tissue engineering applications: Processing related challenges and property assessment, Materials Science and Engineering: R: Reports. 103 (2016) 1–39. https://doi.org/https://doi.org/10.1016/j.mser.2016.01.001.

[83] G. Zhang, H. Chen, S. Yang, Y. Guo, N. Li, H. Zhou, Y. Cao, Frozen slurry-based laminated object manufacturing to fabricate porous ceramic with oriented lamellar structure, J Eur Ceram Soc. 38 (2018) 4014–4019. https://doi.org/https://doi.org/10.1016/j.jeurceramsoc.2018.04.032.

[84] H.W. Tan, T. Tran, C.K. Chua, A review of printed passive electronic components through fully additive manufacturing methods, Virtual Phys Prototyp. 11 (2016) 271–288. https://doi.org/10.1080/17452759.2016.1217586.

[85] S. Jha, M. Velhal, W. Stewart, V. Amin, E. Wang, H. Liang, Additively manufactured electrodes for supercapacitors: A review, Appl Mater Today. 26 (2022). https://doi.org/10.1016/j.apmt.2021.101220.

[86] Z. Wang, Q. Zhang, S. Long, Y. Luo, P. Yu, Z. Tan, J. Bai, B. Qu, Y. Yang, J. Shi, H. Zhou, Z.-Y. Xiao, W. Hong, H. Bai, Three-Dimensional Printing of Polyaniline/Reduced Graphene Oxide Composite for High-Performance Planar Supercapacitor, ACS Appl Mater Interfaces. 10 (2018) 10437–10444. https://doi.org/10.1021/acsami.7b19635.

[87] B. Chen, Y. Jiang, X. Tang, Y. Pan, S. Hu, Fully Packaged Carbon Nanotube Supercapacitors by Direct Ink Writing on Flexible Substrates, ACS Appl Mater Interfaces. 9 (2017) 28433–28440. https://doi.org/10.1021/acsami.7b06804.

[88] Guilve Guo, Sandwiched nanoarchitecture of reduced graphene oxide/ZnO nanorods/reduced graphene oxide on flexible PET substrate for supercapacitor, Appl Phys Lett. 99 (2011).

[89] X. Wu, L. Meng, Q. Wang, W. Zhang, Y. Wang, A flexible asymmetric fibered-supercapacitor based on unique Co3O4@PPy core-shell nanorod arrays electrode, Chemical Engineering Journal. 327 (2017) 193–201. https://doi.org/https://doi.org/10.1016/j.cej.2017.06.096.

[90] J. Orangi, F. Hamade, V.A. Davis, M. Beidaghi, 3D Printing of Additive-Free 2D Ti3C2Tx (MXene) Ink for Fabrication of Micro-Supercapacitors with Ultra-High Energy Densities, ACS Nano. 14 (2020) 640–650. https://doi.org/10.1021/acsnano.9b07325.

[91] X. Li, R. Chen, Y. Zhao, Q. Liu, J. Liu, J. Yu, J. Li, P. Liu, J. Li, J. Wang, Layer-by-layer inkjet printing GO film anchored Ni(OH)2 nanoflakes for high-performance supercapacitors, Chemical Engineering Journal. 375 (2019) 121988. https://doi.org/https://doi.org/10.1016/j.cej.2019.121988.

[92] Y. Gao, X. Guo, Z. Qiu, G. Zhang, R. Zhu, Y. Zhang, H. Pang, Printable electrode materials for supercapacitors, ChemPhysMater. 1 (2022) 17–38. https://doi.org/https://doi.org/10.1016/j.chphma.2021.09.002.

[93] Y. Xu, I. Hennig, D. Freyberg, A. James Strudwick, M. Georg Schwab, T. Weitz, K. Chih-Pei Cha, Inkjet-printed energy storage device using graphene/polyaniline inks, J Power Sources. 248 (2014) 483–488. https://doi.org/https://doi.org/10.1016/j.jpowsour.2013.09.096.

[94] Md Rashedul Islam, Shaila Afroj, Kostya S. Novoselov, Nazmul Karim, Smart Electronic Textile-Based Wearable Supercapacitors, Advanced Science. 9 (2022).

[95] Z. Stempien, M. Khalid, M. Kozanecki, P. Filipczak, A. Wrzesińska, E. Korzeniewska, E. Sąsiadek, Inkjet Printing of Polypyrrole Electroconductive Layers Based on Direct Inks Freezing and Their Use in Textile Solid-State Supercapacitors, Materials. 14 (2021). https://doi.org/10.3390/ma14133577.

[96] C.Y. Foo, H.N. Lim, M.A. Mahdi, M.H. Wahid, N.M. Huang, Three-Dimensional Printed Electrode and Its Novel Applications in Electronic Devices, Sci Rep. 8 (2018) 7399. https://doi.org/10.1038/s41598-018-25861-3.

[97] Zhang CF, Kremer MP, Seral-Ascaso A., Park SH, N. McEvoy, Anasori B, Gogotsi Y, Nicolosi V, Stamping of Flexible, Coplanar Micro-Supercapacitors Using MXene Inks, Adv Funct Mater. 28 (2018).

[98] P. Chang, H. Mei, Y. Tan, Y. Zhao, W. Huang, L. Cheng, A 3D-printed stretchable structural supercapacitor with active stretchability/flexibility and remarkable volumetric capacitance, J Mater Chem A Mater. 8 (2020) 13646–13658. https://doi.org/10.1039/D0TA04460A.

[99] Y. Yang, Z. Chen, X. Song, B. Zhu, T. Hsiai, P.-I. Wu, R. Xiong, J. Shi, Y. Chen, Q. Zhou, K.K. Shung, Three dimensional printing of high dielectric capacitor using projection based stereolithography method, Nano Energy. 22 (2016) 414–421. https://doi.org/https://doi.org/10.1016/j.nanoen.2016.02.045.

[100] B. Rezaei, J.Y. Pan, C. Gundlach, S.S. Keller, Highly structured 3D pyrolytic carbon electrodes derived from additive manufacturing technology, Mater Des. 193 (2020) 108834. https://doi.org/https://doi.org/10.1016/j.matdes.2020.108834.

[101] Y. Zhao, J. Yao, Z. Zhong, Z. Sun, The research of powertrain for supercapacitor-based series hybrid Bus, in: 2008 IEEE Vehicle Power and Propulsion Conference, 2008: pp. 1–4. https://doi.org/10.1109/VPPC.2008.4677450.

[102] X. Lu, T. Zhao, X. Ji, J. Hu, T. Li, X. Lin, W. Huang, 3D printing well organized porous iron-nickel/polyaniline nanocages multiscale supercapacitor, J Alloys Compd. 760 (2018) 78–83. https://doi.org/https://doi.org/10.1016/j.jallcom.2018.05.165.

[103] Adriano Ambrosi, James Guo Sheng Moo, Martin Pumera, Helical 3D-Printed Metal Electrodes as Custom-Shaped 3D Platform for Electrochemical Devices, Adv Funct Mater. 26 (2015).

[104] T. Famprikis, P. Canepa, J.A. Dawson, M.S. Islam, C. Masquelier, Fundamentals of inorganic solid-state electrolytes for batteries, Nat Mater. 18 (2019) 1278–1291. https://doi.org/10.1038/s41563-019-0431-3.

[105] A.J. Blake, R.R. Kohlmeyer, J.O. Hardin, E.A. Carmona, B. Maruyama, J.D. Berrigan, H. Huang, M.F. Durstock, 3D Printable Ceramic–Polymer Electrolytes for Flexible High-Performance Li-Ion Batteries with Enhanced Thermal Stability, Adv Energy Mater. 7 (2017) 1602920. https://doi.org/https://doi.org/10.1002/aenm.201602920.

[106] K. Lee, Y. Shang, V.A. Bobrin, R. Kuchel, D. Kundu, N. Corrigan, C. Boyer, 3D Printing Nanostructured Solid Polymer Electrolytes with High Modulus and Conductivity, Advanced Materials. 34 (2022) 2204816. https://doi.org/https://doi.org/10.1002/adma.202204816.

[107] K.G. Cho, S.S. Jang, I. Heo, H. Kyung, W.C. Yoo, K.H. Lee, 3D printed solid-state composite electrodes and electrolytes for high-energy-density flexible microsupercapacitors, J Energy Storage. 53 (2022) 105206. https://doi.org/https://doi.org/10.1016/j.est.2022.105206.

[108] D.W. McOwen, S. Xu, Y. Gong, Y. Wen, G.L. Godbey, J.E. Gritton, T.R. Hamann, J. Dai, G.T. Hitz, L. Hu, E.D. Wachsman, 3D-Printing Electrolytes for Solid-State Batteries, Advanced Materials. 30 (2018) 1707132. https://doi.org/https://doi.org/10.1002/adma.201707132.

[109] A. Hornés, A. Pesce, L. Hernández-Afonso, A. Morata, M. Torrell, Albert Tarancón, AM of fuel cells, (n.d.).

[110] N.M. Farandos, L. Kleiminger, T. Li, A. Hankin, G.H. Kelsall, Three-dimensional Inkjet Printed Solid Oxide Electrochemical Reactors. I. Yttria-stabilized Zirconia Electrolyte, Electrochim Acta. 213 (2016) 324–331. https://doi.org/https://doi.org/10.1016/j.electacta.2016.07.103.

[111] R.I. Tomov, M. Krauz, J. Jewulski, S.C. Hopkins, J.R. Kluczowski, D.M. Glowacka, B.A. Glowacki, Direct ceramic inkjet printing of yttria-stabilized zirconia electrolyte layers for anode-supported solid oxide fuel cells, J Power Sources. 195 (2010) 7160–7167. https://doi.org/https://doi.org/10.1016/j.jpowsour.2010.05.044.

[112] M. Dudek, R.I. Tomov, C. Wang, B.A. Glowacki, P. Tomczyk, R.P. Socha, M. Mosiałek, Feasibility of direct carbon solid oxide fuels cell (DC-SOFC) fabrication by inkjet printing technology, Electrochim Acta. 105 (2013) 412–418. https://doi.org/https://doi.org/10.1016/j.electacta.2013.04.139.

[113] T.-H. Lee, K.-Y. Liu, F.E. Wiria, P.-C. Su, Inkjet-printed silver and samarium-doped ceria nanocomposite cathode for low temperature solid oxide fuel cells, in: 2017 IEEE/SICE International Symposium on System Integration (SII), 2017: pp. 83–88. https://doi.org/10.1109/SII.2017.8279193.

[114] A. Willert, F.Z. Tabary, T. Zubkova, P.E. Santangelo, M. Romagnoli, R.R. Baumann, Multilayer additive manufacturing of catalyst-coated membranes for polymer electrolyte membrane fuel cells by inkjet printing, Int J Hydrogen Energy. 47 (2022) 20973–20986. https://doi.org/https://doi.org/10.1016/j.ijhydene.2022.04.197.

[115] I. Pchelintsev, R. Karamov, A. Tikhonov, O. Dubinin, I. Shishkovsky, Fabrication of hierarchical lattice structures from zirconia stabilized ceramics by micro-SLA 3D printing approach, Ceram Int. (2023). https://doi.org/https://doi.org/10.1016/j.ceramint.2023.05.264.

[116] A. Tang, L. Crisci, L. Bonville, J. Jankovic, An overview of bipolar plates in proton exchange membrane fuel cells, Journal of Renewable and Sustainable Energy. 13 (2021) 022701. https://doi.org/10.1063/5.0031447.

[117] K.S. Lyons, B.D. Gould, Lightweight Titanium Metal Bipolar Plates for PEM Fuel Cells, Materials Science Forum. 879 (2017) 613–618. https://doi.org/10.4028/www.scientific.net/MSF.879.613.

[118] U. Gulzar, C. Glynn, C. O'Dwyer, Additive manufacturing for energy storage: Methods, designs and material selection for customizable 3D printed batteries and supercapacitors, Curr Opin Electrochem. 20 (2020) 46–53. https://doi.org/https://doi.org/10.1016/j.coelec.2020.02.009.

[119] J. Yan, S. Huang, Y. Von Lim, T. Xu, D. Kong, X. Li, H.Y. Yang, Y. Wang, Direct-ink writing 3D printed energy storage devices: From material selectivity, design and optimization strategies to diverse applications, Materials Today. 54 (2022) 110–152. https://doi.org/https://doi.org/10.1016/j.mattod.2022.03.014.

[120] J. Yan, G. Zhi, D. Kong, H. Wang, T. Xu, J. Zang, W. Shen, J. Xu, Y. Shi, S. Dai, X. Li, Y. Wang, 3D printed rGO/CNT microlattice aerogel for a dendrite-free sodium metal anode, J Mater Chem A Mater. 8 (2020) 19843–19854. https://doi.org/10.1039/d0ta05817c.

[121] Z. Lyu, G.J.H. Lim, J.J. Koh, Y. Li, Y. Ma, J. Ding, J. Wang, Z. Hu, J. Wang, W. Chen, Y. Chen, Design and Manufacture of 3D-Printed Batteries, Joule. 5 (2021) 89–114. https://doi.org/https://doi.org/10.1016/j.joule.2020.11.010.

[122] S. Praveen, G.S. Sim, C.W. Ho, C.W. Lee, 3D-printed twisted yarn-type Li-ion battery towards smart fabrics, Energy Storage Mater. 41 (2021) 748–757. https://doi.org/https://doi.org/10.1016/j.ensm.2021.07.024.

[123] C.L. Cramer, E. Ionescu, M. Graczyk-Zajac, A.T. Nelson, Y. Katoh, J.J. Haslam, L. Wondraczek, T.G. Aguirre, S. LeBlanc, H. Wang, M. Masoudi, E. Tegeler, R. Riedel, P. Colombo, M. Minary-Jolandan, Additive manufacturing of ceramic materials for energy applications: Road map and opportunities, J Eur Ceram Soc. 42 (2022) 3049–3088. https://doi.org/https://doi.org/10.1016/j.jeurceramsoc.2022.01.058.

[124] T. Chu, S. Park, K. (Kelvin) Fu, 3D printing-enabled advanced electrode architecture design, Carbon Energy. 3 (2021) 424–439. https://doi.org/https://doi.org/10.1002/cey2.114.

[125] S. Park, B. Shi, Y. Shang, K. Deng, K. Fu, Structured Electrode Additive Manufacturing for Lithium-Ion Batteries, Nano Lett. 22 (2022) 9462–9469. https://doi.org/10.1021/acs.nanolett.2c03545.

[126] P. Zhu, P.R. Slater, E. Kendrick, Insights into architecture, design and manufacture of electrodes for lithium-ion batteries, Mater Des. 223 (2022) 111208. https://doi.org/https://doi.org/10.1016/j.matdes.2022.111208.

[127] T.-S. Wei, B.Y. Ahn, J. Grotto, J.A. Lewis, 3D Printing of Customized Li-Ion Batteries with Thick Electrodes, Advanced Materials. 30 (2018) 1703027. https://doi.org/https://doi.org/10.1002/adma.201703027.

[128] S.-K. Cho, H.-I. Kim, J.-W. An, K. Jung, H. Bae, J.H. Kim, T. Yim, S.-Y. Lee, Printable Solid Electrolyte Interphase Mimic for Antioxidative Lithium Metal Electrodes, Adv Funct Mater. 30 (2020) 2000792. https://doi.org/https://doi.org/10.1002/adfm.202000792.

[129] T. Chu, S. Park, K. (Kelvin) Fu, 3D printing-enabled advanced electrode architecture design, Carbon Energy. 3 (2021) 424–439. https://doi.org/https://doi.org/10.1002/cey2.114.

[130] S.H. Park, G. Goodall, W.S. Kim, Perspective on 3D-designed micro-supercapacitors, Mater Des. 193 (2020) 108797. https://doi.org/https://doi.org/10.1016/j.matdes.2020.108797.

[131] R. Heimböckel, S. Kraas, F. Hoffmann, M. Fröba, Increase of porosity by combining semi-carbonization and KOH activation of formaldehyde resins to prepare high surface area carbons for supercapacitor applications, Appl Surf Sci. 427 (2018) 1055–1064. https://doi.org/https://doi.org/10.1016/j.apsusc.2017.08.095.

[132] M. Li, S. Zhou, L. Cheng, F. Mo, L. Chen, S. Yu, J. Wei, 3D Printed Supercapacitor: Techniques, Materials, Designs, and Applications, Adv Funct Mater. 33 (2023) 2208034. https://doi.org/https://doi.org/10.1002/adfm.202208034.

[133] B. Yao, S. Chandrasekaran, J. Zhang, W. Xiao, F. Qian, C. Zhu, E.B. Duoss, C.M. Spadaccini, M.A. Worsley, Y. Li, Efficient 3D Printed Pseudocapacitive Electrodes with Ultrahigh MnO2 Loading, Joule. 3 (2019) 459–470. https://doi.org/https://doi.org/10.1016/j.joule.2018.09.020.

[134] C. Lin, Y.-F. Zhang, D. Lu, A. Silva, Z. Liu, H.Y. Yang, Low-Temperature Resistant Stretchable Micro-Supercapacitor Based on 3D Printed Octet-Truss Design, Small. 19 (2023) 2207634. https://doi.org/https://doi.org/10.1002/smll.202207634.

[135] M.M. Ovhal, N. Kumar, H.B. Lee, B. Tyagi, K.-J. Ko, S. Boud, J.-W. Kang, Roll-to-roll 3D printing of flexible and transparent all-solid-state supercapacitors, Cell Rep Phys Sci. 2 (2021) 100562. https://doi.org/https://doi.org/10.1016/j.xcrp.2021.100562.

[136] Y. Zhao, F. Liu, Z. Zhao, P. Bai, Y. Ma, A. Alhadhrami, G.A.M. Mersal, Z. Lin, M.M. Ibrahim, Z.M. El-Bahy, Direct ink printing reduced graphene oxide/KCu7S4 electrodes for high-performance supercapacitors, Adv Compos Hybrid Mater. 5 (2022) 1516–1526. https://doi.org/10.1007/s42114-022-00488-1.

[137] S.A. Rasaki, C. Liu, C. Lao, H. Zhang, Z. Chen, The innovative contribution of additive manufacturing towards revolutionizing fuel cell fabrication for clean energy generation: A comprehensive review, Renewable and Sustainable Energy Reviews. 148 (2021) 111369. https://doi.org/https://doi.org/10.1016/j.rser.2021.111369.

[138] A. Pesce, A. Hornés, M. Núñez, A. Morata, M. Torrell, A. Tarancón, 3D printing the next generation of enhanced solid oxide fuel and electrolysis cells, J Mater Chem A Mater. 8 (2020) 16926–16932. https://doi.org/10.1039/D0TA02803G.

[139] B. Xing, Y. Yao, X. Meng, W. Zhao, M. Shen, S. Gao, Z. Zhao, Self-supported yttria-stabilized zirconia ripple-shaped electrolyte for solid oxide fuel cells application by digital light processing three-dimension printing, Scr Mater. 181 (2020) 62–65. https://doi.org/https://doi.org/10.1016/j.scriptamat.2020.02.004.

[140] M.C. Bermúdez Agudelo, M. Hampe, T. Reiber, E. Abele, Investigation of Porous Metal-Based 3D-Printed Anode GDLs for Tubular High Temperature Proton Exchange Membrane Fuel Cells, Materials. 13 (2020). https://doi.org/10.3390/ma13092096.

[141] W. Lai, Y. Wang, Z. Lei, R. Wang, Z. Lin, C.-P. Wong, F. Kang, C. Yang, High performance, environmentally benign and integratable Zn//MnO2 microbatteries, J Mater Chem A Mater. 6 (2018) 3933–3940. https://doi.org/10.1039/C7TA10936A.

[142] C.M. Costa, R. Gonçalves, S. Lanceros-Méndez, Recent advances and future challenges in printed batteries, Energy Storage Mater. 28 (2020) 216–234. https://doi.org/https://doi.org/10.1016/j.ensm.2020.03.012.

[143] S. Peng, Q. Guo, N. Thirunavukkarasu, Y. Zheng, Z. Wang, L. Zheng, L. Wu, Z. Weng, Tailoring of photocurable ionogel toward high resilience and low hysteresis 3D printed versatile porous flexible sensor, Chemical Engineering Journal. 439 (2022) 135593. https://doi.org/https://doi.org/10.1016/j.cej.2022.135593.

[144] Y. Yang, W. Yuan, X. Zhang, Y. Yuan, C. Wang, Y. Ye, Y. Huang, Z. Qiu, Y. Tang, Overview on the applications of three-dimensional printing for rechargeable lithium-ion batteries, Appl Energy. 257 (2020) 114002. https://doi.org/https://doi.org/10.1016/j.apenergy.2019.114002.

[145] Frank Markus, Can 3D Printing Finally Make Solid-State EV Batteries Practical?, (2023).

[146] A. Tarancón, V. Esposito, M. Torrell, M. Di Vece, J.S. Son, P. Norby, S. Barg, P.S. Grant, A. Vogelpoth, S. Linnenbrink, M. Brucki, T. Schopphoven, A. Gasser, E. Persembe, D. Koufou, S. Kuhn, R. Ameloot, X. Hou, K. Engelbrecht, C.R.H. Bahl, N. Pryds, J. Wang, C. Tsouris, E. Miramontes, L. Love, C. Lai, X. Sun, M.R. Kærn, G. Criscuolo, D.B. Pedersen, 2022 roadmap on 3D printing for energy, JPhys Energy. 4 (2022). https://doi.org/10.1088/2515-7655/ac483d.

[147] R.S. Haridas, A. Gumaste, P. Varshney, B.R. Manu, K. Kandasamy, N. Kumar, R.S. Mishra, SolidStir Additive Manufacturing: A Novel Deformation-Based Additive Manufacturing Using Friction Stir Technology, JOM. (2023). https://doi.org/10.1007/s11837-023-06063-3.

[148] Y. Zhou, C.B. Parker, P. Joshi, A.K. Naskar, J.T. Glass, C. Cao, 4D Printing of Stretchable Supercapacitors via Hybrid Composite Materials, Adv Mater Technol. 6 (2021). https://doi.org/10.1002/admt.202001055.

[149] L. Gao, R. Fan, W. Zhou, X. Hu, K. Cao, W. Wang, Y. Lu, Biomimetic and Radially Symmetric Graphene Aerogel for Flexible Electronics, Adv Electron Mater. 5 (2019) 1900353. https://doi.org/https://doi.org/10.1002/aelm.201900353.

[150] M. Wang, D. Vecchio, C. Wang, A. Emre, X. Xiao, Z. Jiang, P. Bogdan, Y. Huang, N.A. Kotov, Biomorphic structural batteries for robotics, Sci Robot. 5 (2020) eaba1912. https://doi.org/10.1126/scirobotics.aba1912.

[151] T. Prater, J. Edmunsson, M. Fiske, F. Ledbetter, C. Hill, M.D. Meyyappan, C. Roberts, L. Huebner, P. Hall, N. Werkheiser, NASA's In-Space Manufacturing Project: Update on Manufacturing Technologies and Materials to Enable More Sustainable and Safer Exploration, 2019.

[152] A. Maurel, A.C. Martinez, D.A. Dornbusch, W.H. Huddleston, M.-L. Seol, C.R. Henry, J.M. Jones, B. Yelamanchi, S. Bakhtar Chavari, J.E. Edmunson, S.T. Sreenivasan, P. Cortes, E. MacDonald, C.G. Sherrard, What Would Battery Manufacturing Look Like on the Moon and Mars?, ACS Energy Lett. 8 (2023) 1042–1049. https://doi.org/10.1021/acsenergylett.2c02743.

[153] J. Wadsworth, C.S. Cockell, Perchlorates on Mars enhance the bacteriocidal effects of UV light, Sci Rep. 7 (2017) 4662. https://doi.org/10.1038/s41598-017-04910-3.

[154] Y. Wang, S. Song, C. Xu, N. Hu, J. Molenda, L. Lu, Development of solid-state electrolytes for sodium-ion battery–A short review, Nano Materials Science. 1 (2019) 91–100. https://doi.org/https://doi.org/10.1016/j.nanoms.2019.02.007.